ADVANCING EARTH AND SPACE SCIENCES

JGR Atmospheres

RESEARCH ARTICLE
10.1029/2026JD046686

Different Last Millennium El Niño Southern Oscillation Sea Surface Temperature Patterns Drive Disparate North Atlantic Tropical Cyclone Characteristics

Elizabeth Wallace[1], Sylvia Dee[2], Andrew Bierbower[2], Xinyue Luo[2], Richard Sullivan[1,3], Wenchang Yang[4,5], Gabe Vecchi[4], and Kerry Emanuel[6]

[1]Department of Earth and Ocean Science, Old Dominion University, Norfolk, VA, USA, [2]Department of Earth, Environmental, and Planetary Sciences, Rice University, Houston, TX, USA, [3]Center for Catastrophe Modeling and Resilience, Lehigh University, Lehigh, PA, USA, [4]Department of Geosciences, Princeton University, Princeton, NJ, USA, [5]High Meadows Environmental Institute, Princeton University, Princeton, NJ, USA, [6]Program in Atmospheres, Oceans, and Climate, Department of Earth, Atmospheric, and Planetary Sciences, Massachusetts Institute of Technology, Cambridge, MA, USA

Key Points:

- Three last millennium simulations yield different Central Pacific and Eastern Pacific El Nino sea surface temperature patterns
- There is no consistent response in Atlantic tropical cyclones to diverse El Nino events across different last millennium simulations
- We need to improve simulation of diverse El Nino events in climate models to properly characterize their impacts on extreme events

Supporting Information:

Supporting Information may be found in the online version of this article.

Correspondence to:

E. Wallace,
ejwallac@odu.edu

Citation:

Wallace, E., Dee, S., Bierbower, A., Luo, X., Sullivan, R., Yang, W., et al. (2026). Different last millennium El Niño Southern oscillation sea surface temperature patterns drive disparate North Atlantic tropical cyclone characteristics. *Journal of Geophysical Research: Atmospheres*, *131*, e2026JD046686. https://doi.org/10.1029/2026JD046686

Received 18 FEB 2026
Accepted 8 SEP 2026

Author Contributions:

Conceptualization: Elizabeth Wallace, Sylvia Dee, Xinyue Luo
Data curation: Elizabeth Wallace, Sylvia Dee, Wenchang Yang, Kerry Emanuel
Formal analysis: Elizabeth Wallace, Sylvia Dee, Andrew Bierbower, Xinyue Luo, Richard Sullivan
Funding acquisition: Elizabeth Wallace, Sylvia Dee, Xinyue Luo, Gabe Vecchi, Kerry Emanuel

Abstract

Understanding the relationship between the El Niño-Southern Oscillation (ENSO) phenomenon and North Atlantic tropical cyclone (TC) activity is critical for both seasonal predictions and future projections of TCs. Unfortunately, the satellite observational era (1970-present) captures too few El Niño events to fully characterize the response of TC activity to this multivariate, multi-scalar, and non-linear climate phenomenon. Here we explore ENSO-TC teleconnections using large data sets (>100 k) of synthetic North Atlantic tropical cyclones simulated for the past millennium using three different climate reconstructions - two earth system models (Max Planck Institute, Community Earth System Model) and one paleoclimate data assimilation reconstruction (Last Millennium Reanalysis v2.1). El Niño events contain different "flavors," ranging from canonical events characterized by warming in the Eastern Pacific (EP) to Central Pacific (CP) events with warming concentrated in the equatorial CP. Each last millennium reconstruction produces different warming patterns for CP and EP El Niño events. These differences result in a lack of a consistent response in TC genesis, track, or intensity during each type of event. In general, El Niño events suppress storms in the North Atlantic across models, but the patterns of suppression are largely model dependent. Our work highlights a need for improving simulations of realistic CP and EP El Niño sea surface temperature patterns to properly characterize North Atlantic TC risks in a changing climate.

Plain Language Summary

North Atlantic tropical cyclones annually impact coastlines in North America, the Caribbean, and Central America damaging coastal properties and ecosystems and threatening human lives. Sea surface temperature warming patterns in the tropical Pacific Ocean known as El Niño events act to suppress North Atlantic TC activity. There are different flavors of El Niño events with warming concentrated in either the central or eastern Pacific Ocean (called CP and EP events). It is unclear how tropical cyclones respond to diverse El Niño warming patterns due to our short observational record of this natural hazard. We analyze large data sets of North Atlantic tropical cyclones produced using three different climate simulations of the past 1,000 years. We find that each climate simulation represents ocean warming in the Pacific differently for CP and EP El Niño years. These differing El Niño warming patterns across simulations result in a lack of coherent response in the North Atlantic TC patterns. Our results highlight a need for making improvements in the simulation of El Niño events across climate models. Without accurate and consistent ocean warming patterns, it is difficult to understand the response of natural hazards like tropical cyclones to these climate events.

1. Introduction

North Atlantic tropical cyclones (TCs) pose a substantial risk to populated coastlines in North America, the Caribbean, and Central America as well as to marine activities and ecosystems. TCs are affected by natural modes of climate variability that shift oceanic and atmospheric conditions (ocean temperatures, steering winds, etc.) where storms form and travel (Goldenberg & Shapiro, 1996; Kossin et al., 2010; Ting et al., 2019). Climate models that contain future warming in the eastern tropical Pacific (El Niño-like behavior) show different TC projections for the 21st century compared to models that contain future cooling in the eastern tropical Pacific (La

Investigation: Elizabeth Wallace, Andrew Bierbower, Xinyue Luo, Richard Sullivan
Methodology: Elizabeth Wallace, Sylvia Dee, Xinyue Luo, Richard Sullivan, Kerry Emanuel
Project administration: Elizabeth Wallace, Sylvia Dee, Xinyue Luo, Gabe Vecchi, Kerry Emanuel
Resources: Elizabeth Wallace, Gabe Vecchi, Kerry Emanuel
Software: Elizabeth Wallace, Wenchang Yang, Kerry Emanuel
Supervision: Elizabeth Wallace, Sylvia Dee, Xinyue Luo, Gabe Vecchi
Validation: Elizabeth Wallace, Wenchang Yang
Visualization: Elizabeth Wallace
Writing – original draft: Elizabeth Wallace, Sylvia Dee, Xinyue Luo
Writing – review & editing: Elizabeth Wallace, Sylvia Dee, Andrew Bierbower, Xinyue Luo, Richard Sullivan, Wenchang Yang, Gabe Vecchi, Kerry Emanuel

Niña-like behavior) (Lin et al., 2025). Therefore, it is important to understand the response of TCs to changing sea surface temperatures (SSTs) in the tropical Pacific.

ENSO affects cyclogenesis in the North Atlantic through SST and wind shear feedbacks (Camargo et al., 2007; Gray, 1984; Lin et al., 2021). A warm-phase ENSO (El Niño) event increases upper-tropospheric westerly winds and vertical wind shear (VWS) in the tropical North Atlantic, which inhibits the formation and growth of TCs (Chu, 2004; Goldenberg & Shapiro, 1996). El Niño events also promote warmer tropical SSTs in the Pacific, which leads to upper-tropospheric warming (Tang & Neelin, 2004) and cooler tropical relative SSTs in the North Atlantic, setting up less favorable conditions for TC genesis (Villarini et al., 2010). Relative humidity decreases during El Niño years, promoting fewer storms in the Atlantic (Camargo et al., 2007). A cool phase of ENSO (La Niña) favors more TC activity in the North Atlantic with weaker VWS and warmer tropical relative SSTs in the North Atlantic (Lin et al., 2021).

There is substantial variability in the patterns, amplitudes, and centers of maximum warming/cooling during ENSO events (Capotondi et al., 2015). No two ENSO events are alike, and variations in SST result in atmospheric forcing that is variable for any given event (Capotondi et al., 2021; Wyrtki, 1975). Typically, ENSO events (see Capotondi et al., 2015 for a review) are sorted into two specific styles: CP El Niño events and EP El Niño events. Both event types are named for their locus of maximum warming. Based off the short observational interval, a "canonical" El Niño event (EP El Niño) is characterized by SSTs reaching maximum values along the western coast of South America and decreasing in magnitude moving westward along the equator (Rasmusson & Carpenter, 1982). Central Pacific (CP) El Niños typically have weaker SST anomalies and peak near 180-160°W with less warming in the EP (Capotondi et al., 2015). There is large natural variability in the frequency of EP or CP El Niño events in the context of the last millennium, but the 20th century has seen a shift toward stronger EP El Niños (Luo et al., 2022). Model simulations of the 21st century suggest CP El Niño events will occur more frequently, and EP El Niño events are likely to become stronger (Lee & McPhaden, 2010; Yeh et al., 2009).

Although there is evidence that the structure of ENSO events impacts teleconnections over land (e.g., Ashok et al., 2007; Larkin & Harrison, 2005a, 2005b), less work has constrained how variable CP and EP SST patterns affect TC characteristics. Two studies (Mueller et al., 2024; Patricola et al., 2016) explored the connections between diverse ENSO phases and Atlantic TCs in historical and future climate using TC-permitting dynamical modeling (e.g., the Weather Research and Forecasting [WRF] model). Patricola et al. (2016) analyzed TC response to composites of the strongest observed EP and CP El Niño SST patterns, including an idealized doubled CP El Niño SST pattern (Lee & McPhaden, 2010). EP El Niño SST patterns contributed to more Atlantic TC suppression than CP El Niño SSTs of the same magnitude. Increased TC suppression during EP El Niño years resulted from circulation changes that enhanced VWS over the Atlantic. This modeling work takes important first steps toward understanding the dynamical controls affecting TCs during diverse El Niño events but is limited to the use of a single climate model (Community Earth System Model, CESM) and idealized SST patterns based on the brief 20th-century observations. We have not observed enough diverse El Niño events to fully characterize TC response to these events in a statistically meaningful way. The 20th century only contains 10 CP El Niño events (Yu & Zou, 2013)– all with slightly different characteristics. To robustly analyze how decadal and longer time scales of climate variability influence TC characteristics, we need more than the available 50 years of observations.

Here, we use a large ensemble of statistical dynamically downscaled TCs (Sullivan et al., 2025a; Wallace, Dee, & Emanuel, 2021a, 2021b) spanning the past millennium and present climate (850–2005 CE) using three complementary climate data sets including two earth system model simulations, Max Planck Institute Earth System Model (MPI-ESM, Giorgetta et al., 2013) and the CESM Last Millennium Ensemble (CESM-LME, Otto-Bliesner et al., 2016), and a paleoclimate data assimilation product, the Last Millennium Reanalysis (LMR version 2.1, Hakim et al., 2016; Tardif et al., 2019). All three of these products yield hundreds of thousands of storms concurrent with multiple different mean climate states that span hundreds of unique ENSO events. We test the hypothesis that CP El Niño events suppress fewer Atlantic hurricanes than EP El Niño events (Mueller et al., 2024; Patricola et al., 2016). We focus on the following questions.

- How did CP and EP El Niño events evolve over the last millennium, and how did this impact the frequency of storms in the North Atlantic?
- What are the spatial and temporal distributions of storm characteristics during CP and EP El Niño events, as well as during La Niña events?

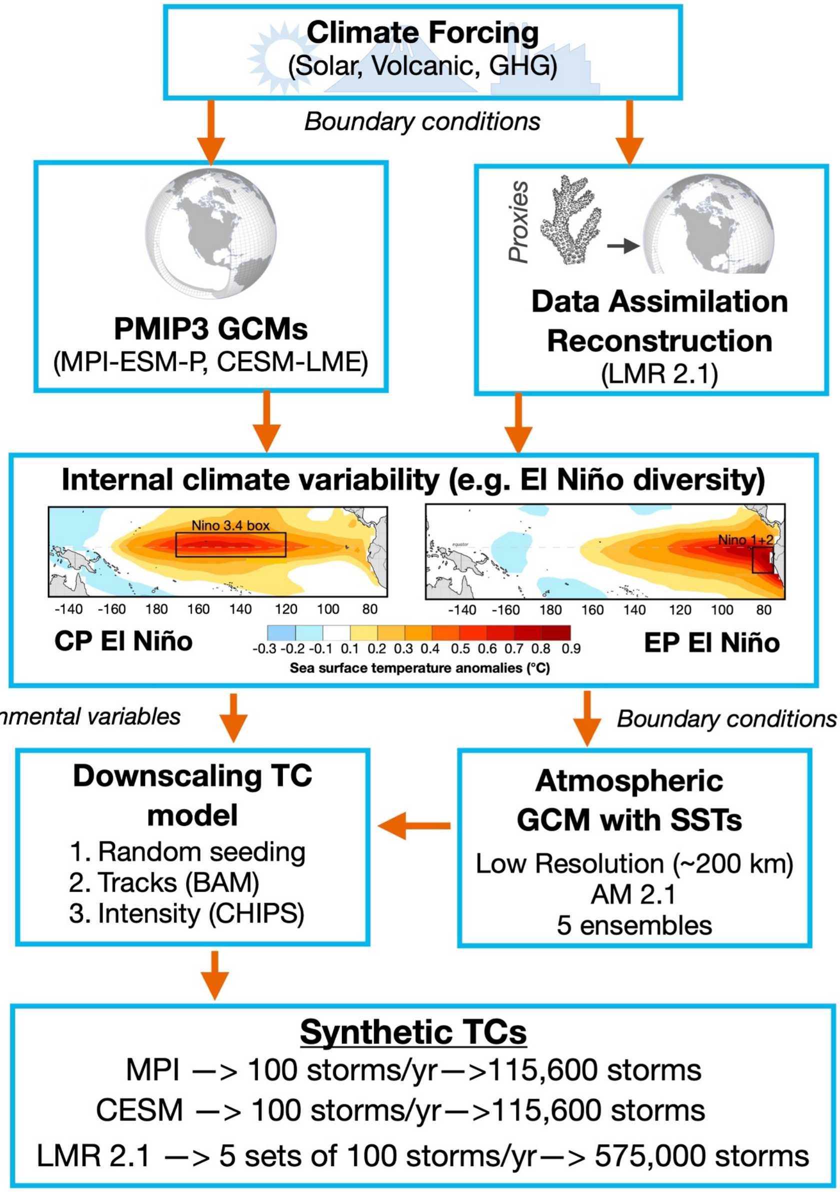

Figure 1. Workflow for generating statistically downscaled storm sets. Storms are generated from climate simulations of the past millennium produced using PMIP3 global climate models (GCMs) and a data assimilation reconstruction. "Canonical" El Nino patterns are shown.

- Do the three last millennium data products—two climate models and one paleoclimate data assimilation product—show consistent ENSO-TC impacts, or not? What key differences exist, and why?

2. Methods and Data Sets

2.1. Climate Model and Paleoclimate Reanalysis Data Sets

Our workflow (Figure 1) follows two steps: (a) extract relevant climate variables (e.g., SSTs, winds) for the last millennium from simulations, and (b) run a TC model using these climate variables as input to generate TC tracks and frequency estimates. We use three data products that simulate or reconstruct last millennium climate: the Max Planck Institute Earth System Model (MPI-ESM; Giorgetta et al., 2013), the Community Earth System Model-Last Millennium Ensemble (CESM-LME full forcing ensemble #7; Otto-Bliesner et al., 2016), and the Last Millennium Reanalysis (LMR v2.1; Tardif et al., 2019). Importantly, MPI and CESM-LME are the only two sets

10.1029/2026JD046686

of ensemble climate model simulations from the Paleoclimate Modeling Intercomparison Project Phase three (PMIP3) (Braconnot et al., 2012; PAGES 2k-PMIP3 group, 2015) that provide daily wind data for the last millennium, critical for running the TC model. We compare our results from each climate model to a coupled reanalysis product for the last century (CERA-20C; Laloyaux et al., 2018). All data sets and their SST biases are described in Section S1 in Supporting Information S1.

LMR2.1 is fundamentally different from the two climate models (CESM and MPI) used in this work. It provides a field reconstruction in which the spatial information is derived from a climate model, but the *temporal evolution is derived solely from paleoclimate proxies* at annual resolution (Hakim et al., 2016; Tardif et al., 2019). Thus, LMR provides a more realistic reconstruction of low-frequency climate variability (Yang et al., 2024). Any externally forced climate signals contained in LMR emerge only due to the temporal evolution of the paleoclimate data network, whereas CESM and MPI are transiently forced with last millennium boundary conditions. LMR offers a closer glimpse into "real" world climate than traditional GCMs (i.e., PMIP3) by integrating paleoclimate proxies into GCM simulations. To generate the atmospheric inputs needed for downscaling TCs, we coupled an atmospheric GCM (GFDL-AM2.1; GFDL Global Atmospheric Model Development Team, 2004) with SSTs supplied from combining the observed SST climatology (ERA5; Hersbach et al., 2020) with LMR-based annual SST anomalies (Sullivan et al., 2025a). The use of the observed SST climatology likely mitigates some of the impacts of mean-state biases that degrade the simulation of ENSO-TC connections (Vecchi et al., 2014).

2.2. Storm Data Sets

For each reconstruction of the last millennium (CESM, MPI: 850–2005 CE; LMR: 850–1999 CE), we used a large database (100 storms/year) of synthetic tropical cyclones (Sullivan et al., 2025a; Wallace et al., 2021a, 2021b) generated using a statistically-dynamically downscaled TC model (Emanuel et al., 2006, 2008). Storm totals for each last millennium simulation include 115,600, 115,600, and 575,000 (115,000 × five ensembles) for CESM, MPI, and LMR 2.1, respectively (Figure 1). TCs range from tropical storms to Category 5 intensity (wind speeds from 34 to 135 knots). For a detailed description of the TC downscaling methodology, see Section S2 in Supporting Information S1.

We compared TC frequency, intensity, and accumulated cyclone energy (ACE; Bell & Chelliah, 2006) during ENSO years. The annual TC frequency is calculated as a target of 100 surviving storms divided by the number of storms seeded to achieve this target for each year of the model simulation (i.e., MPI, CESM, LMR), calibrated to match the observational TC frequency from 1970 to 2005 CE. Accumulated Cyclone Energy for a hurricane season is calculated as the sum of the squares of the estimated 6-hourly maximum sustained wind speed (knots) for all TCs while they are at least tropical storm strength. Differences in storm properties across ENSO years were assessed using a Welch's t-test. For understanding spatial shifts in storms, we also calculated annual genesis density and track density in a 5 by 5-degree grid. We use a bootstrapping method with 100 samples. We randomly sample with replacement from CP years only and EP years only to calculate genesis density and track density in each type of El Niño year. We applied a Wilcoxon rank sum test (95% threshold) to compare the actual genesis and track density values with the bootstrapped values to assess the statistical significance of the storm density patterns.

2.3. Methods for Identifying ENSO Events

El Niño/La Niña events are defined with the Niño 3.4 index. First, a 30-year running mean is removed to calculate SST anomalies (SSTA). The Niño 3.4 index is computed using SSTA averaged over the Niño 3.4 region (5°S–5°N, 170–120°W). We define El Niño (La Niña) years when the August-September (ASO) Niño 3.4 index anomalies exceed +1 standard deviation (−1 standard deviation) (Bamston et al., 1997; Kousky & Higgins, 2007). The standard deviations to define ENSO events for LMR were computed using a 30-year moving window to account for the reduction of variance in LMR SSTs in the early part of the record (Luo et al., 2022).

Each El Niño year was sorted into a CP or EP event using the C and E index method (Takahashi et al., 2011). The "C" and "E" indices are computed with a linear combination of the first two principal components of tropical Pacific SSTA (30°S–30°N, 120°E–80°W), projecting a 45°-rotated orthogonal coordinate:

$$C = (PC1 + PC2)/\sqrt{2}, E = (PC1 - PC2)/\sqrt{2}$$

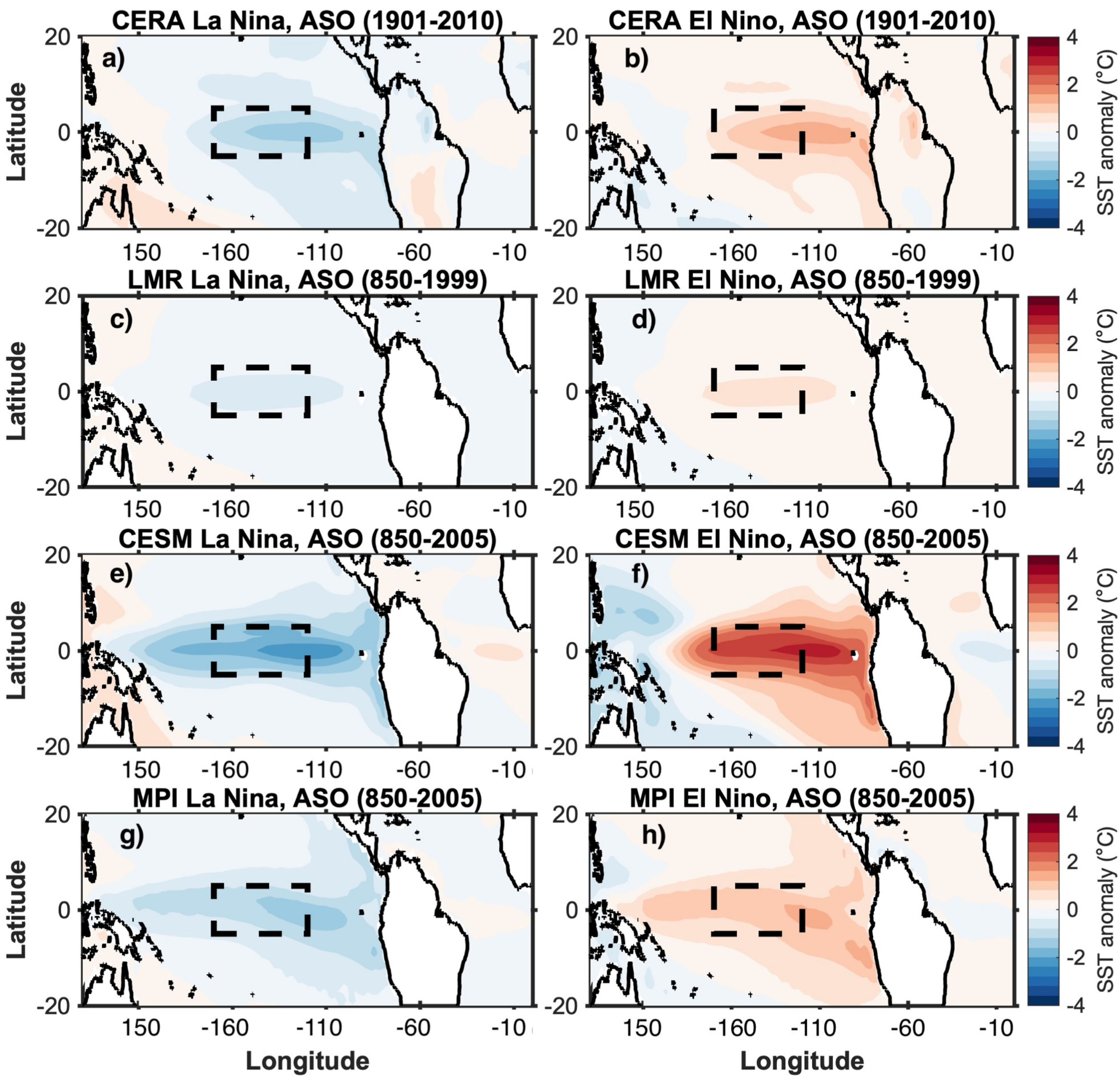

Figure 2. Average sea surface temperature (SST) patterns for La Niña (a, c, e, g) and El Niño (b, d, f, h) years in August-September-October (ASO) for CERA (a, b), LMR (c, d), CESM (e, f), and MPI (g, h). Color contours show the SST anomaly in degrees Celsius. Black dashed box outlines the Niño3.4 region. Note that each data product spans a different number of years, indicated in figure panel titles.

If the ASO value of the E index is higher in a given El Niño year than the C index, then that El Niño year is categorized as an EP El Niño year, and vice versa for the CP El Niño years. CESM, MPI, and LMR contained 123, 101, and 85 EP events, respectively; 47, 72, and 103 CP events, respectively; and 148, 175, and 197 La Niña events over the past millennium, respectively.

3. Results

3.1. SST Patterns: El Niño and La Niña

We examined SST patterns associated with La Niña, CP El Niño, and EP El Niño in all three last millennium data sets (Figures 2 and 3). For La Niña (Figure 2), cool SST anomalies in MPI and CESM extend further west (~150°E) than in the two reanalysis products, CERA and LMR (170°E). The location of the maximum SST cooling is similar in all models centered around 110–150°W (Figures 2a, 2c, 2e and 2g). For El Niño, LMR SST

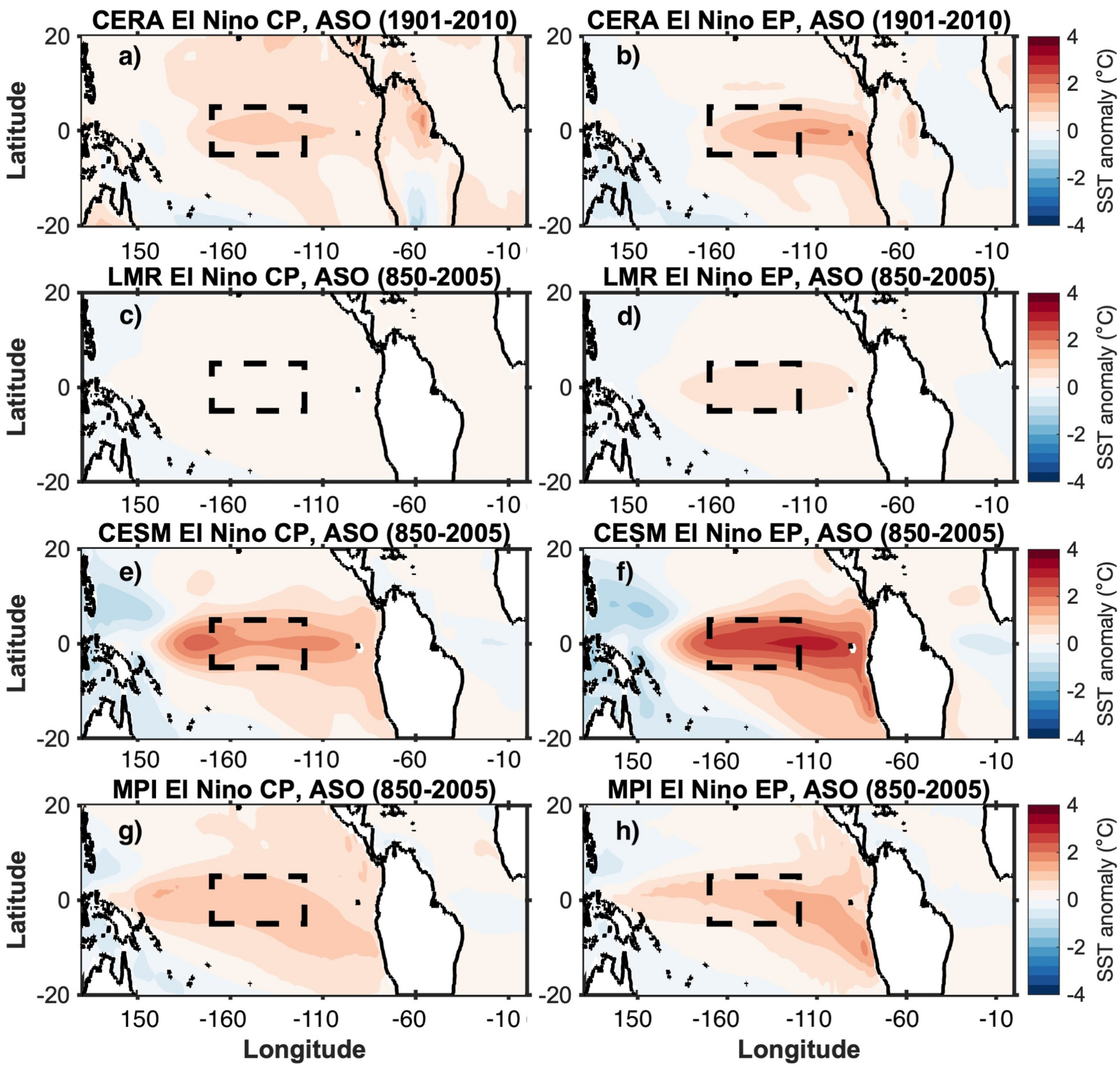

Figure 3. Same as Figure 2 but for Central Pacific (a, c, e, g) and Eastern Pacific (b, d, f, h) El Niño years.

anomalies peak in the Niño3.4 region (black dashed box in Figure 2d). CERA, MPI, and CESM El Niño SST anomalies peak slightly east of the Niño3.4 region (Figures 2b, 2f and 2h). The magnitude of ENSO warming in CESM is much larger (2–4°C) (Figure 2f) than CERA, LMR, and MPI, which show 0.3–1.5°C warming during El Niño events (Figures 2b, 2d and 2h).

3.2. SST Patterns: EP and CP El Niño

The EP and CP patterns identified by applying the C and E index (Section 2.3) to all four data products show notable differences. CERA shows EP/CP El Niño SST patterns closer to the "canonical" pattern (Figure 1), with muted CP warming centered in the Niño3.4 region (Figure 3a) and a strong EP warming pattern closer to ~110°W and extending along the South American coastline (Figure 3b). In CESM and MPI, CP events produce a western bias in the SST anomaly maxima (Figures 3e and 3g). In MPI, CP SST anomalies reach Papua New Guinea. In MPI and CESM, EP events show distinct patterns of warming from CP events. MPI EP events peak further east with higher SSTs extending along the South American coastline (Figure 3h); CESM shows EP events with broad warming in the Niño3.4 region extending toward South America (Figure 3f). There are few differences in SST anomalies between LMR CP and EP events, only larger magnitude warming in the Niño3.4 region during EP events (Figures 3c and 3d).

The differences in SSTs that emerge across all four data sets highlight the issues of using a binary CP and EP classification for the LMR data set (Luo et al., 2022). Indeed, the patterns of warming themselves (rather than the value of index time series) are critical for understanding the impacts on teleconnected regions (Luo et al., 2022, 2023) and on Atlantic TCs (Mueller et al., 2024; Williams & Patricola, 2018).

3.3. The Timing of CP and EP Events Across Models/Pattern of Warming

We evaluated how CP and EP events evolve in the four climate reconstructions, counting the total number of events in a 50-year moving window (Figure 4). In LMR, CP events are more common than EP events over most of the past millennium. However, in the last 300 years (1700–2000), LMR climate shifts toward more EP events. In MPI, there are similar numbers of CP and EP events throughout the duration of the simulation; CP events hover around approximately three events per 50 years, and EP events at approximately four events per 50 years (Figure 4b). There are a few multi-decadal periods where EP events dominate in MPI last millennium climate (e.g., 1550–1600 CE, 1750–1850 CE). In CESM, EP events dominate for the full simulation, with an average of five EP events and two CP events per 50 years (Figure 4c). All full forcing ensembles of the CESM-LME exhibit a similar pattern of dominance of EP events compared to CP events (Stevenson et al., 2019). There is large natural variability in the frequency of EP and CP El Niño events in all data products, but also interesting tendencies in the models toward more CP (LMR) or EP (MPI, CESM) events. Like LMR, our modern reanalysis product (CERA) shows more EP events than CP events over the last century, with a rising number of EP events from 1950 to 2010. The individual event years in each simulation (un-binned) are plotted in Figure S1 in Supporting Information S1.

3.4. Genesis and Track Density Patterns Across Models

TCs respond differently to EP and CP warming events across climate simulations. In the MPI-ESM climate, CP years generally produce more Atlantic TCs than EP years. CP warming events correspond to more storms forming in the tropical Atlantic and Caribbean Sea, making landfall along the North American coastline (Figures 5i and 6i).

LMR 2.1 climate creates very little change in genesis density during EP versus CP El Nino years (Figure 5f). Like MPI, there are patterns of elevated track density in the southwest Caribbean Sea with more storms making landfall in Central America and along the Yucatan Peninsula as well as more storms in the northwest Atlantic (Figures 5f and 6f).

Like LMR 2.1 climate, there is very little difference in genesis density patterns across ENSO years in CESM-LME (Figure 5i). For track density (Figure 6i), CP years produce fewer storms that form in the eastern tropical Atlantic and recurve into the northwest Atlantic Ocean and more TCs making landfall in the Gulf of Mexico/Caribbean Sea.

Our reanalysis storm set (CERA-20C) generally shows more storms forming and tracking in the Gulf of Mexico and along the US East Coast in CP El Niño years compared to EP El Niño years (Figure 6c). More storms form in the northwest Atlantic and Caribbean Sea in CP years (Figure 5c), resulting in increased storm landfalls in the Gulf of Mexico and U.S. Southeast (Figure 6c). The magnitude of the track density change observed by the reanalysis storm sets is higher than all three past millennium climate products (Figure 6).

3.5. Accumulated Cyclone Energy (ACE), Intensity, and Frequency

Storm maximum intensity shows no statistically significant change during ENSO years of any type in any of the three data products (Figures 7d–7f). By contrast, all models show a statistically significant shift in TC frequency: there are more storms during La Niña years in the North Atlantic and fewer in El Niño years compared to all years (Figures 7g–7i). CERA (Figure S2c in Supporting Information S1) and LMR (Figure 7a) produce fewer storms during EP years compared to CP years, while CESM and MPI shows similar numbers of storms in EP and CP years (Figures 7b and 7c). The frequency shifts in EP and CP years in CESM and MPI are not statistically different, and the median frequency values for all El Niño events are very similar.

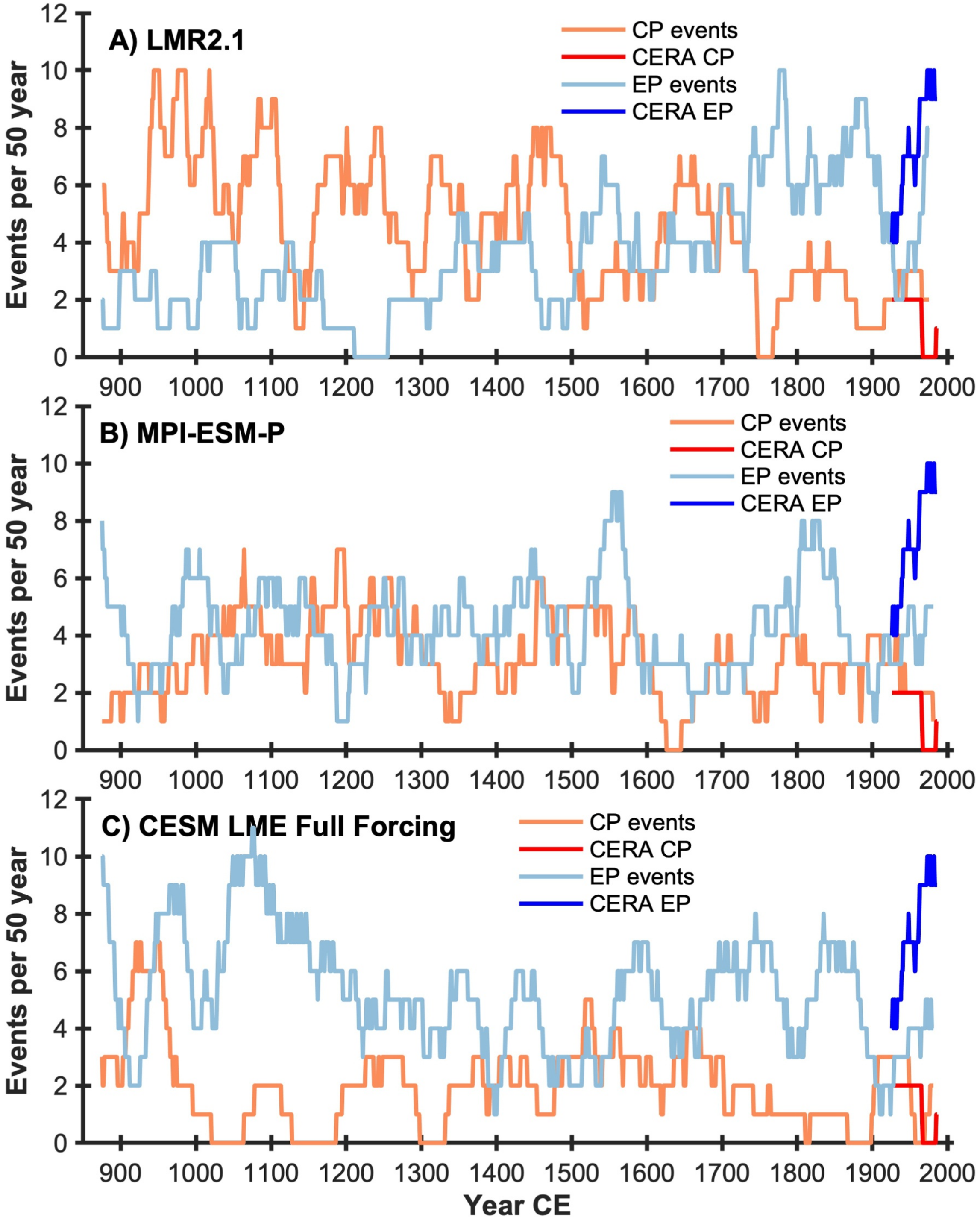

Figure 4. 50-year moving averages for the number of El Niño events over the past millennium (850–2005) for LMRv2.1 (a), MPI-ESM-P (b), and CESM LME (c). On each panel, the 50-year running count of El Niño events in CERA-20C is also shown. El Niño events are sorted into EP (blue) and CP (red) events.

The ACE index suggests that storms are more destructive in La Niña years and less destructive in El Niño years compared to all years in CESM and LMR 2.1 climate (Figures 7a and 7b). Shifts in ACE values during La Niña years for CERA and MPI climate are not statistically significant (Figure 7c, Figure S2a in Supporting Information S1). CESM, MPI and LMR all show less destructive storms during EP El Niño years compared to all years (Figures 7a–7c).

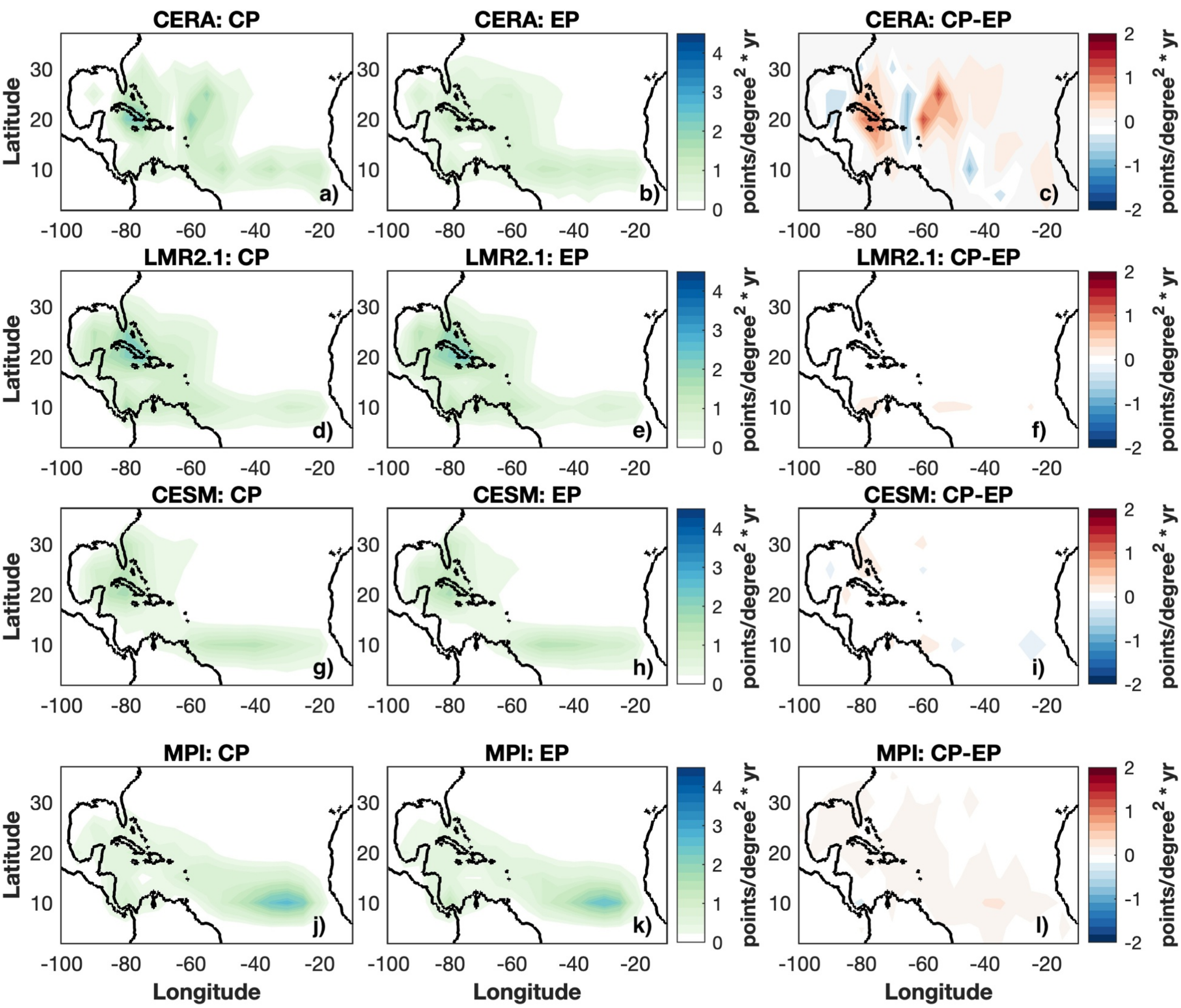

Figure 5. Genesis density (5-degree resolution) for synthetic tropical cyclones during Central Pacific (CP) (a, d, g, j) and Eastern Pacific (EP) (b, e, h, k) years. Difference in genesis density in CP El Niño years minus EP El Niño years (c, f, i, l). All values plotted are statistically significant (0.05 level, Wilcoxon rank sum test). Results are shown for four different data products: CERA (a, b, c), LMR2.1 (d, e, f), CESM (g, h, i), and MPI (j, k, l).

3.6. Mean State SST and Deep Convection Across Models

We analyzed the threshold behavior of tropical deep convection with respect to SST in each last millennium climate product (Figure 8). Deep convection occurs over areas where SSTs are warmest (Waliser et al., 1993) and SST gradients are weak (Sabin et al., 2013). The climatology for all three simulations shows a clear western Pacific warm pool and an eastern equatorial cold tongue (Figure 8). Mean state SST and climatological deep convection show different patterns across climate products. Mean state SSTs in LMR and MPI (Figures 8a and 8g) are characterized by a western Pacific warm pool (defined using 28°C isotherm) which extends to 155°W north of the equator and a cold tongue (defined with 24°C isotherm) that extends to ∼140°W. In CESM (Figure 8d), the warm pool extends much further east in the north hemisphere (140°W) than in MPI or LMR climate, but the CESM equatorial cold tongue has a similar longitudinal extent (140°W) as the other two climate products.

The SST differences across climate products set up different patterns of deep convection in the mean state. Mid-tropospheric (500 hPa) vertical motion indicates deep convection along the coast of Papua New Guinea and concentrated at 160°W in LMR (Figure 8a). In CESM, deep convection is concentrated north of the equator and

10.1029/2026JD046686

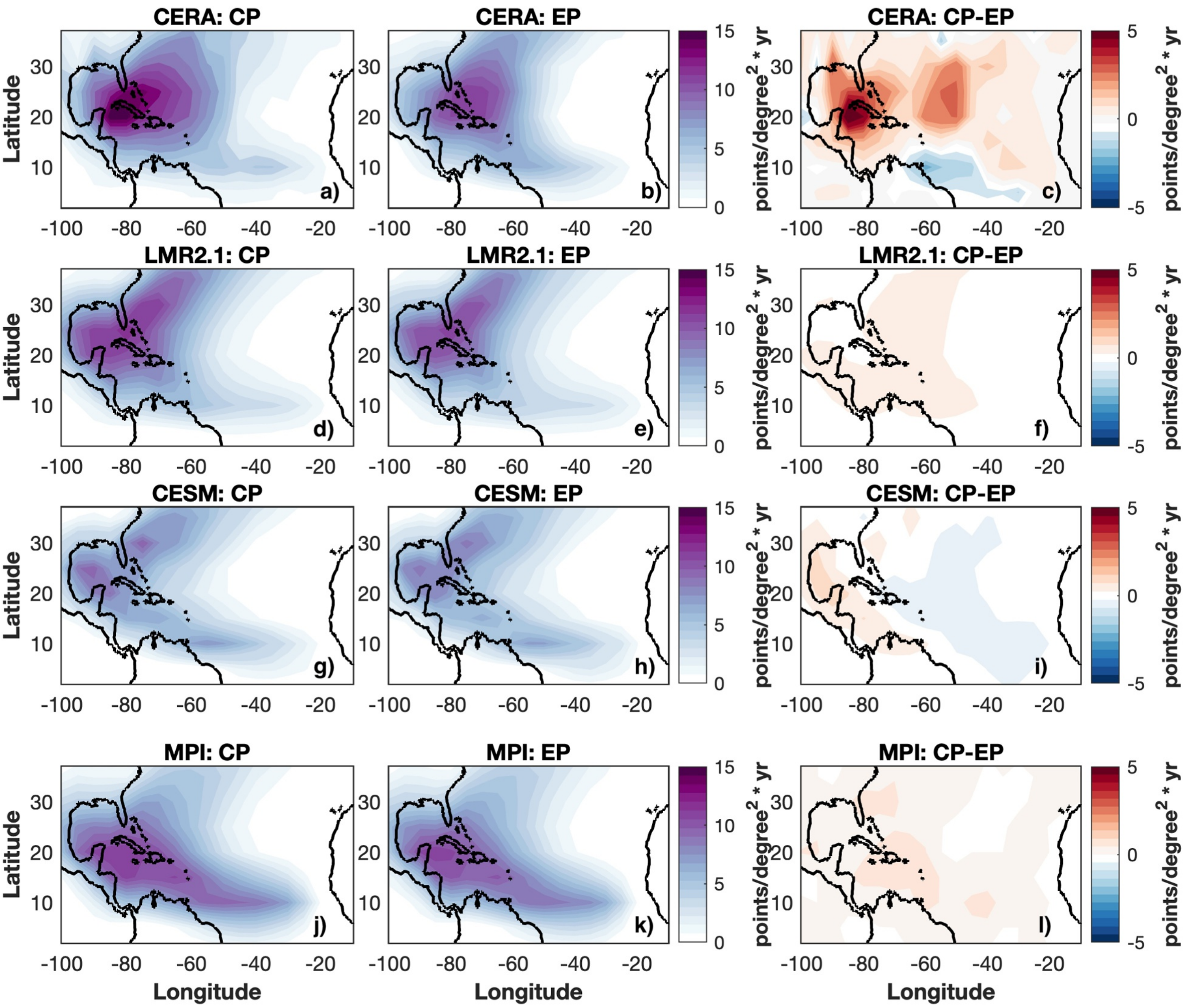

Figure 6. Same as Figure 5 but for track density.

much farther east (100–160°W) than LMR climate (Figure 8d). MPI climatology consists of strong 500 hPa vertical motion from 140°E to 160°W in the northern hemisphere and along the west coast of Mexico (Figure 8g).

There are not strong differences in SSTs or mid-tropospheric circulation comparing CP years to EP years in LMR. Both types of El Niño events result in an eastward shift of the warm pool and a corresponding eastward shift in deep convection both north of the equator and off the coast of Papau New Guinea (Figures 8b and 8c). MPI climate produces an eastward shift in the warm pool by approximately 10° in CP El Niño years. EP El Niño years show a similar spatial extent in the warm pool to the mean state. Both EP and CP years produce a southeastward extension of deep convection in the western Pacific (Figures 8h and 8i). CESM EP and CP years produce a substantial eastward extension of the western Pacific warm pool with ASO SSTs rising above 28°C across the entire basin (Figures 8e and 8f). The eastern equatorial cold tongue (defined by the 24°C isotherm) retracts substantially (reaching 120°W and 110°W in CP and EP years, respectively). In CP and EP years, a zone of deep convection forms in the western Pacific in the northern hemisphere (140–160°E).

3.7. Dynamical Differences Across Models: Vertical Wind Shear (VWS), Potential Intensity (PI), and Relative Humidity

We explored the differences in vertical wind shear (VWS—difference between 850 hPa and 250 hPa), potential intensity (PI) and relative humidity (at 700 hPa) during the peak of the hurricane season (ASO). As expected, in

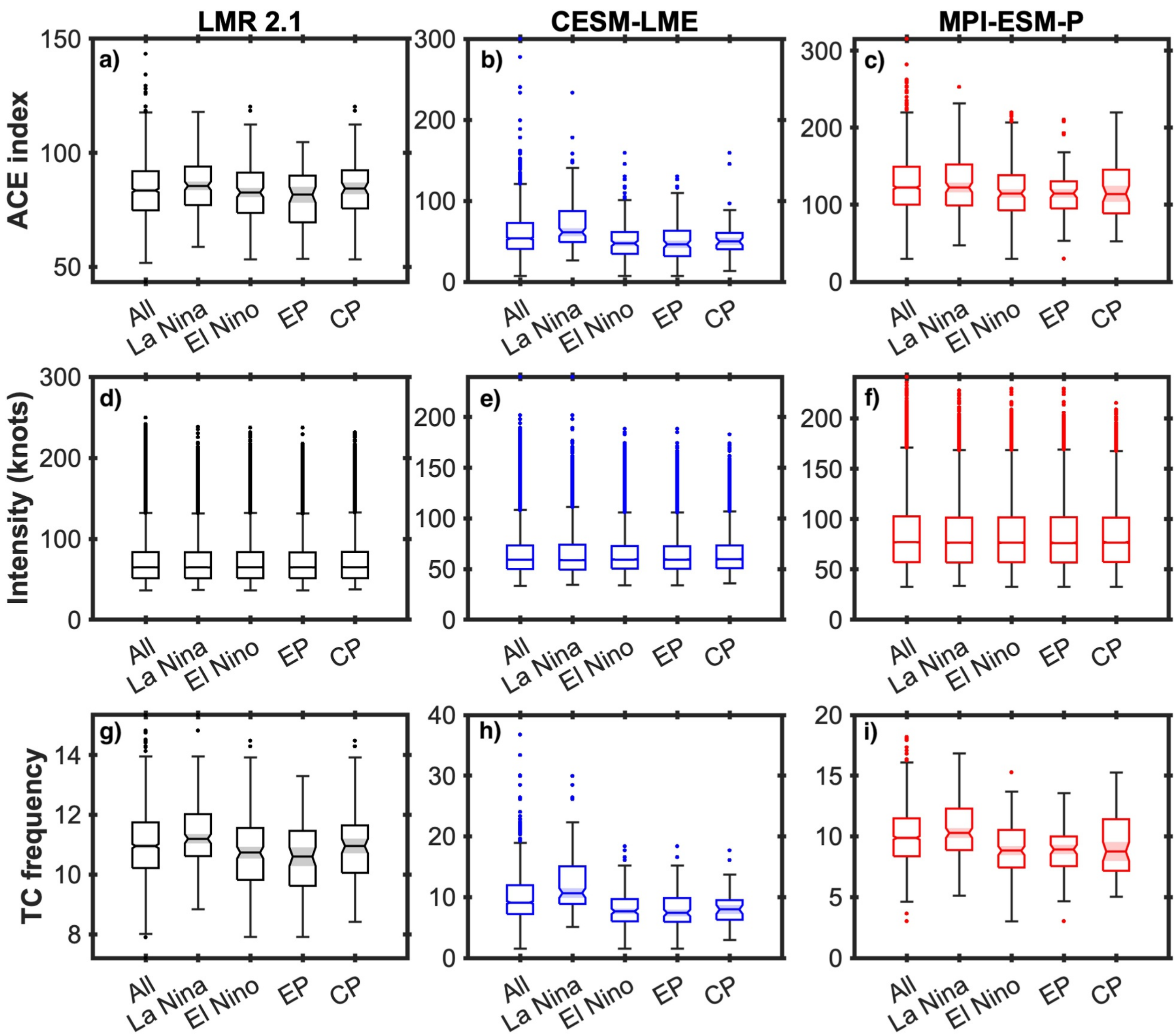

Figure 7. Boxplots of accumulated cyclone energy (ACE) index values (ACE), maximum storm intensity (knots), and storm frequency in all years, La Niña, El Niño, Central Pacific El Niño, and Eastern Pacific El Niño years for three different climate products (MPI (a, d, g), CESM (b, e, h), LMR (c, f, i)) for the past millennium (850–2005 CE). Notches show the 95% confidence intervals for median values.

La Niña years (Figure 9), VWS is lower throughout the North Atlantic in all three last millennium reconstructions. Similarly, relative humidity is higher in all data products in the Caribbean Sea (Figure 10). In contrast, PI is lower for much of the North Atlantic during La Nina years in all three data products with a small patch of higher PI in the southern Caribbean Sea (Figure 11). Lower PI corresponds to generally lower SSTs found in the North Atlantic in all last millennium climate products during La Nina years (Figure 2). The combination of lower VWS and higher humidity favors storm formation and growth in the North Atlantic during La Niña years. Changes in all three variables are more pronounced in the CESM and MPI climate than in the LMR climate (Figures 9–11).

LMR climate shows no appreciable differences in PI, VWS or relative humidity in CP and EP El Niño years compared to the background climate (Figures 9–11). MPI climate, on the other hand, indicates higher VWS (Figure 9h), lower relative humidity (Figure 10h), and lower PI (Figure 11h) in the southern Caribbean Sea during EP El Niño years. These conditions are unfavorable for storm formation, potentially explaining the lower track density (Figure 6l) observed in MPI over the southern Caribbean Sea and Gulf of Mexico during EP El Niño years compared to CP El Niño years.

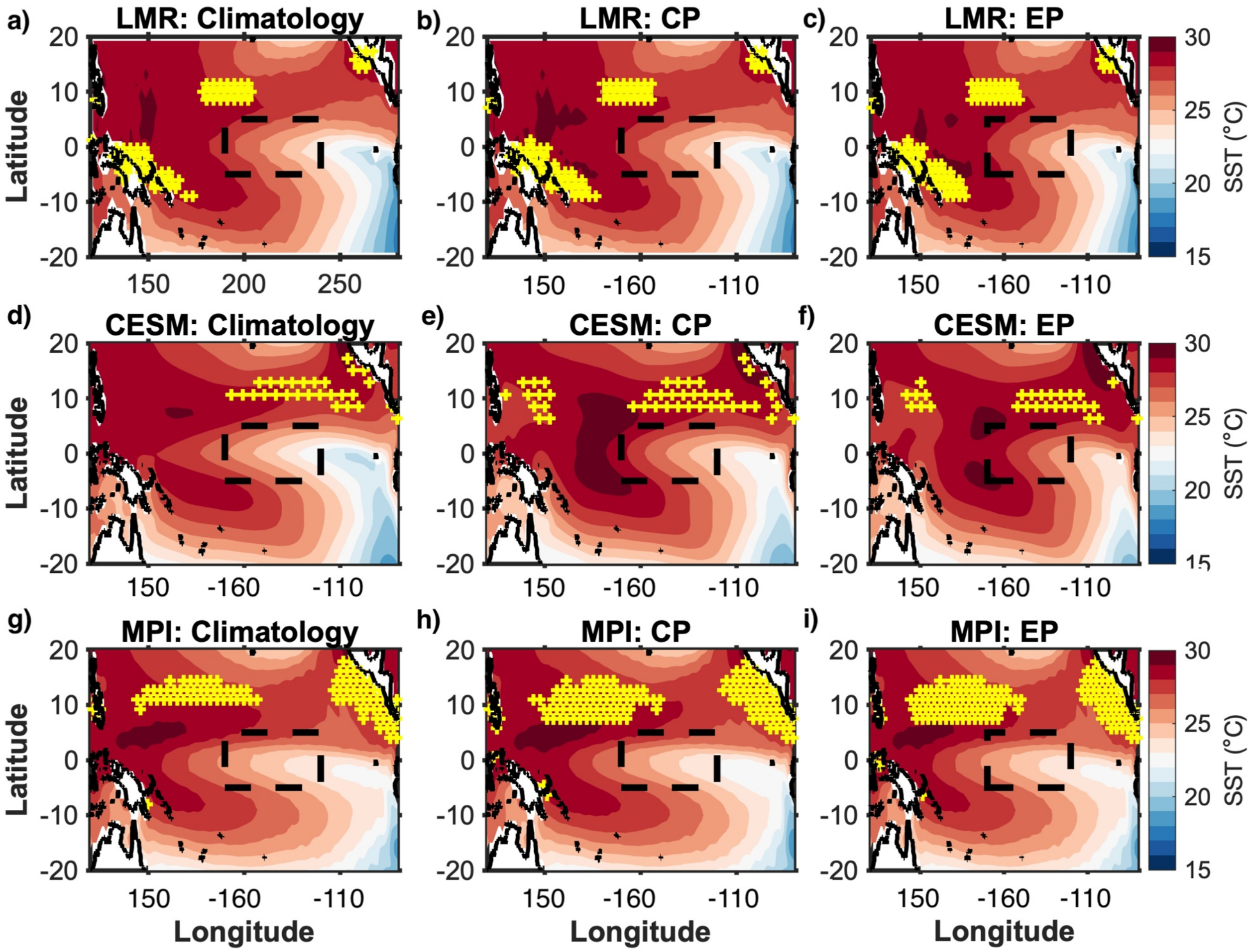

Figure 8. Mean sea surface temperature (°C; color shading) and vertical velocity at 500 hPa (cm/s; yellow hatches; only values exceeding 0.75 cm/s) for MPI, CESM and LMR during all years (a, d, g), Central Pacific El Niño (b, e, h), and Eastern Pacific El Niño (c, f, i) years. All values are from August–October (ASO).

In the CESM climate, both types of El Niño events promote increased VWS over the southern Caribbean, promoting storm suppression in El Niño years (Figures 9d and 9g). The extent and intensity of the VWS increase is larger in EP El Niño years compared to CP El Niño years extending throughout the Gulf of Mexico and along the U.S. East Coast (Figure 9g). Higher VWS in the Gulf of Mexico during EP years explains why there are more storms forming and tracking in the southern Caribbean and Gulf during CP El Niño years within CESM compared to EP El Niño years (Figure 6i). CESM climate shows similar patterns of high relative humidity over the Main Development Region (MDR: 10°–20°N, 20°–60°W) during CP El Niño years and EP El Niño years, which encourage TC formation. In CP and EP years, PI in the MDR increased, creating conditions favorable for TCs. The magnitude and extent of PI increase in the Atlantic is larger during EP years compared to CP years (Figures 11d and 11g), likely contributing to the relative fewer numbers of storms in CP years in the northwest Atlantic in CESM climate (Figure 6i). While PI is a necessary component for TC formation and growth, it is not sufficient. In CESM, the impact of increased VWS over the Gulf of Mexico and U.S. East Coast promote more storms along the Gulf Coast during CP El Niño years compared to EP El Niño year. Similarly, the higher humidity and PI found in the tropical Atlantic in EP years promotes more storms in the northwest Atlantic (Figure 6i).

4. Discussion

There is a critical need to consider the influence of climate variability on TC risk in long-term planning and decision-making, such as how and where properties and infrastructure are developed (Gori et al., 2022). Without a longer record of TCs, we cannot improve our understanding of internal and forced variability in TCs at decadal to centennial timescales. This paper uses three independent data products spanning at least the last 1,000 years and a

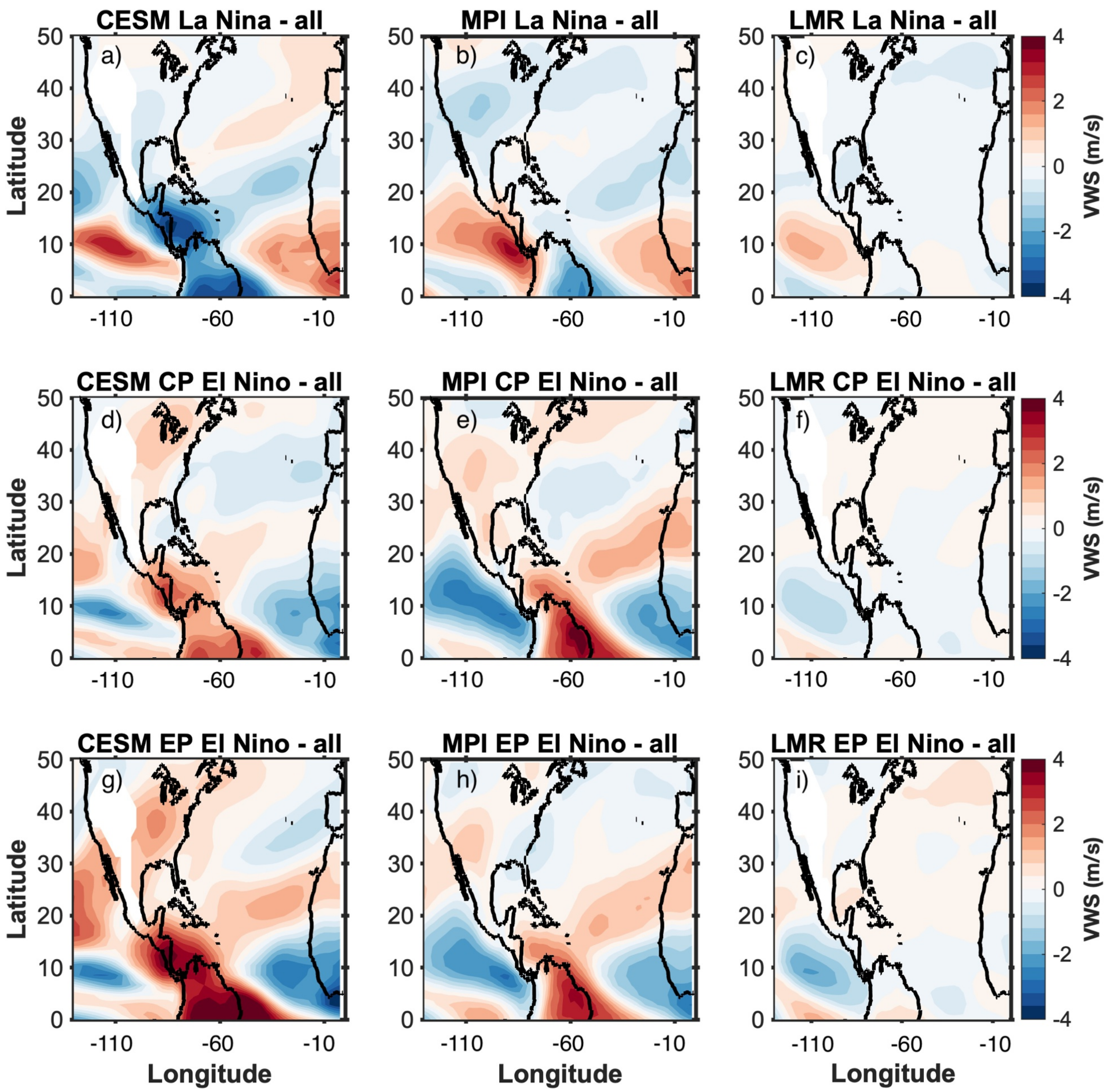

Figure 9. Difference in the ASO zonal 850–250-hPa vertical wind shear (m/s) from La Niña (a, b, c), Central Pacific El Niño (d, e, f), and Eastern Pacific El Niño (g, h, i) years minus all years for CESM (a, d, g), MPI (b, e, h), and LMR 2.1 (c, f, i) past millennium climate.

modern reanalysis data set spanning the last 100 years to investigate how the tropical Pacific climate affects Atlantic TC characteristics. With hundreds of additional realizations of ENSO events, we provide a more robust sample pool of TC characteristics in response to diverse tropical Pacific patterns and amplitudes. The use of multiple climate models and paleoclimate reanalyzes allows us to further explore the dependence of our results on model structural differences, tropical Pacific and Atlantic climate biases, and different representations of multidecadal variability—all of which give rise to important differences in TC climate.

4.1. Divergent TC Climate in Response to ENSO Flavors

We posed three key questions in this work: (a) How do CP and EP El Niño events evolve over the last millennium? (b) What are the spatial and temporal distributions of North Atlantic TC characteristics during ENSO events (CP and EP El Niño, La Niña)? (c) Do the three last millennium data products—two climate models and

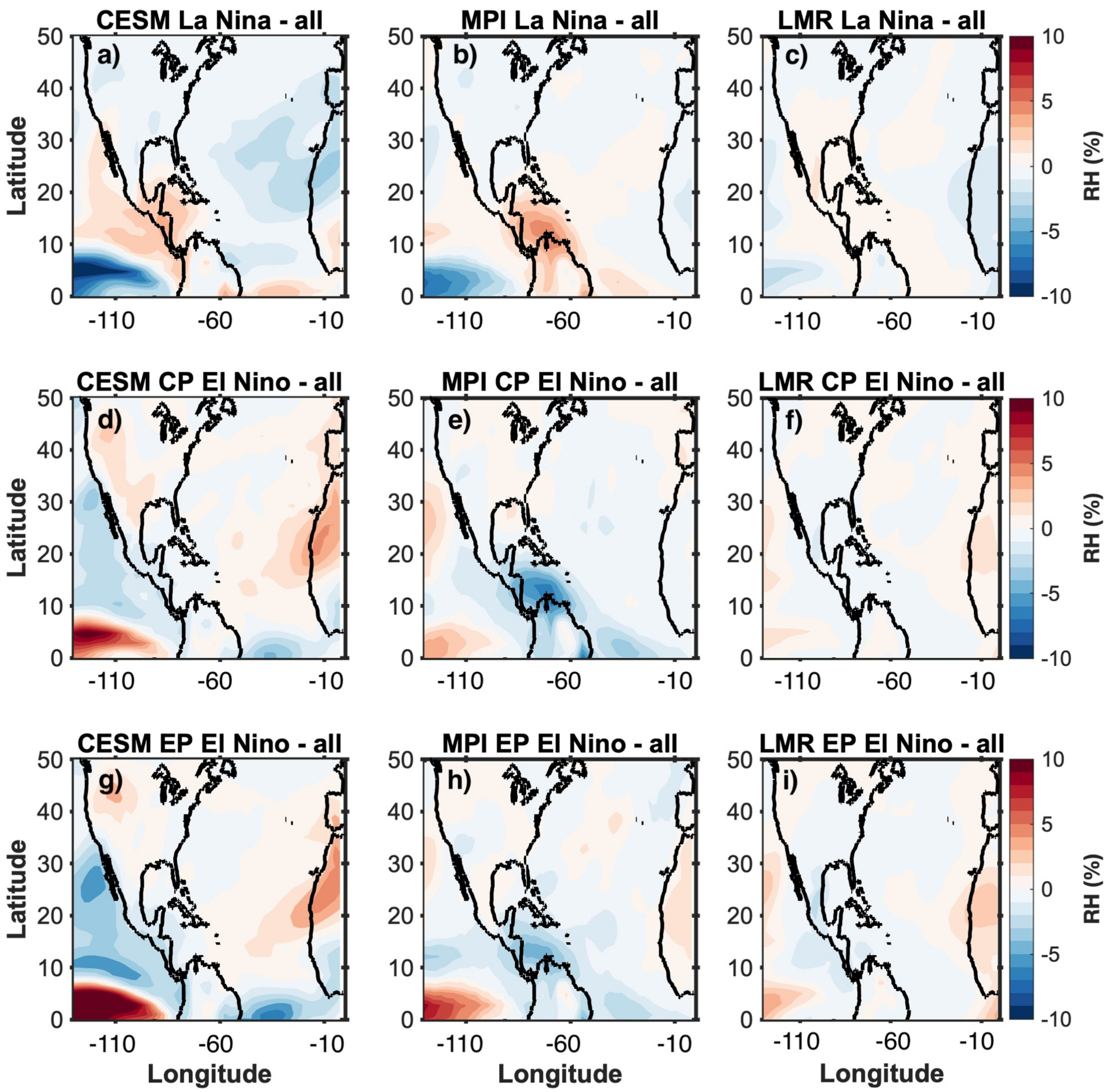

Figure 10. Same as Figure 9 but for ASO 700 hPa relative humidity (%).

one paleoclimate data assimilation product—show consistent ENSO-TC impacts? What key differences exist, and why?

Exploring the SST patterns across the hundreds of ENSO events simulated by our three last millennium climate products, we found consistent differences in TC characteristics between El Niño and La Niña events. La Niña years have more frequent and destructive TCs in the North Atlantic (Figure 7). All simulations successfully capture the appropriate physical mechanisms for the ENSO-TC teleconnection - namely, changes in VWS and relative humidity in response to shifts in tropical Pacific deep convection. The response of TC characteristics to La Niña events was broadly consistent across storm sets for the past millennium even though each data product contained a different tropical Pacific SST response during La Niña years (Figure 2). CESM produced the strongest and most westward shifted tropical Pacific cooling signal (Figure 2e) resulting in much lower VWS in the Atlantic (Figure 9a). While MPI and LMR do show lower VWS (Figures 9b and 9c), this pattern is smaller in magnitude. All three climate reconstructions showed higher relative humidity in the southern Caribbean during

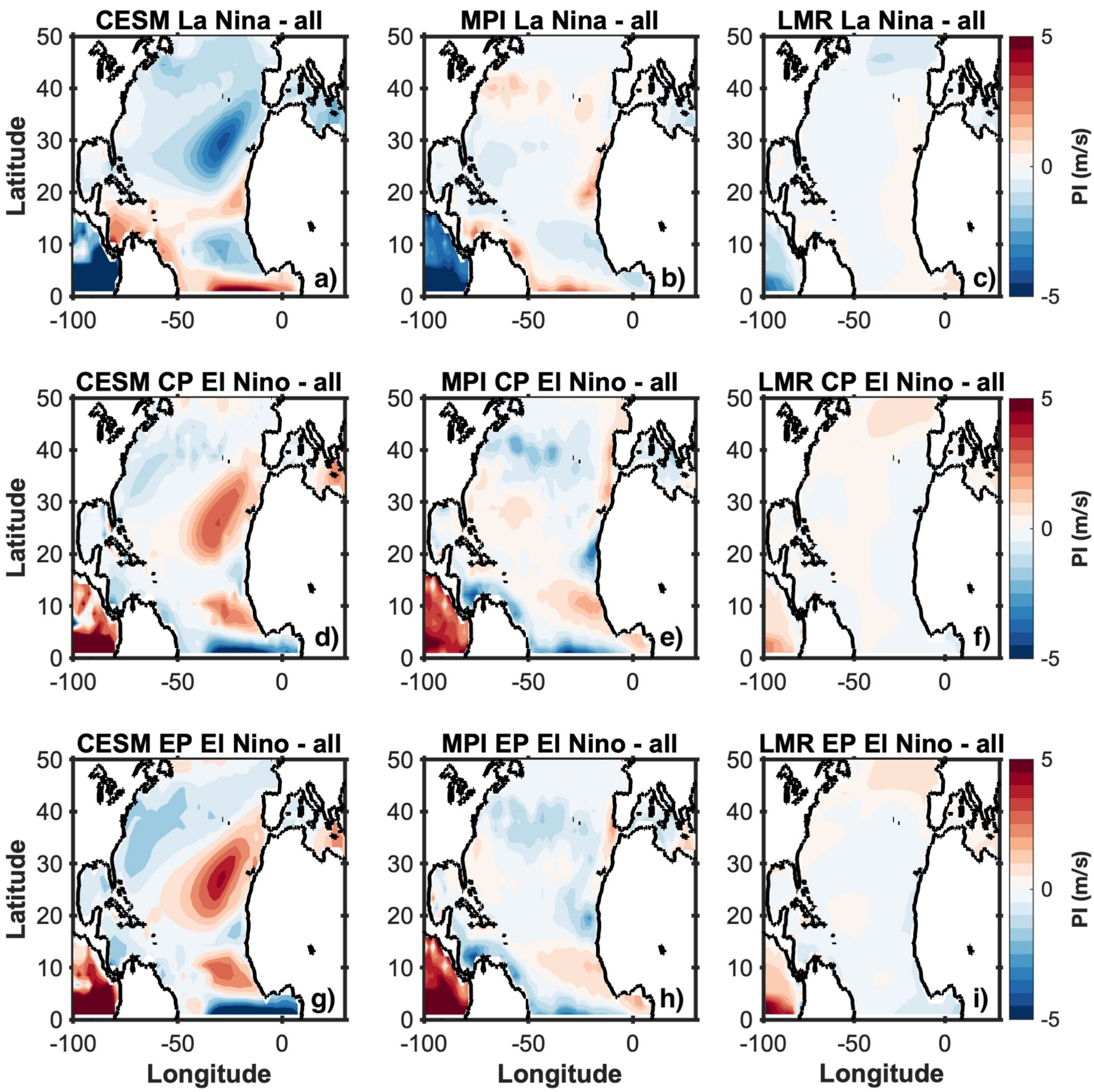

Figure 11. Same as Figure 9 but for ASO potential intensity (m/s).

La Nina years (Figures 10a–10c) with MPI climate containing the largest magnitude increase (Figure 10b). PI generally declined across simulations in La Niña years (Figures 11a–11c) in response to declines in North Atlantic SSTs (Figure 2) and is thus unlikely to be a strong contributing factor to the observed increase in TC frequency and ACE.

There is no consistent response across any of the TC variables we analyzed during CP versus EP El Niño events. Both types of El Niño events suppress storms in the North Atlantic, but the patterns of suppression are model dependent (Figures 5–7). Track density maps suggest that all last millennium climate products produce a tendency toward Gulf landfalling storms during CP events compared to EP events (Figure 6). The number and timing of CP and EP events simulated in all data products also differ widely (Figure 4), with some models showing a predominance of EP events (e.g., CESM) and others showing more CP events (e.g., LMR).

The noisy TC characteristics during EP and CP events, and the lack of agreement across the four data products we analyzed, could be due to many factors, all of which likely culminate in inconsistent TC simulations. First, ENSO SST patterns are different among all data products (Figures 2 and 3). The tropical Pacific SST pattern fundamentally sets the dynamics that produce a TC teleconnection (e.g., relative humidity, VWS, PI, Figures 9–11); therefore, it is unsurprising that the data products yield different outcomes for CP and EP events. All three past millennium climate products showed very different loci for tropical deep convection (as indicated by mid-tropospheric vertical motion). CESM background climate produces the furthest eastward extent of the western pacific warm pool (Figure 8) and the largest eastward shifts in the warm pool extent during CP and EP El Niño's. Warm pool eastward shifts simultaneously lead to tropical deep convection located further east. Previous work (Patricola et al., 2016) has shown that an eastward extension of deep convection contributes to stronger VWS in the tropical Atlantic through changes in the Walker Circulation. Our work indicated a strong VWS response to EP and CP events in CESM climate. LMR climate showed little change in warm pool or deep convection location during EP and CP events (Figure 8) and subsequently had the smallest response in North Atlantic VWS (Figure 9).

There are also differences in the frequencies of CP and EP events across data products. MPI has a more balanced number of CP and EP events, while CESM simulates a larger number of EP events compared to CP (Figure 4). The total number of events in our sample likely affects our results for each data product and its simulated TC climate. Finally, ENSO SST pattern differences alone are unlikely to explain all differences in synthetic TC climates across models and reanalysis products. Other factors, like North Atlantic SST patterns (Patricola et al., 2014; Ting et al., 2019; Yang et al., 2024) and random variability (Kortum et al., 2024), could contribute to inter-model differences in TC climate. LMR, a data assimilation product that likely provides a more reliable reconstruction of internal variability in SSTs and their temporal evolution (Tardif et al., 2019), shows no significant differences between CP and EP events.

We are left with a challenging answer to our last question: Do the models show consistent ENSO-TC impacts? What key differences exist between data products, and why? Without consistent results across models, it is difficult to propose a framework for using a CP/EP event classification system to better predict TC activity in our changing 21st-century climate. Indeed, GCM projections suggest EP events will strengthen in a warming climate, and that CP events may become more frequent (Cai et al., 2018; Shin et al., 2022). Even if we assume these projections are correct, using these ENSO projections to more accurately project future TC climate may not yet be possible. Moreover, our analysis of four data products suggests reliance on a single model or reanalysis for TC projections is likely insufficient.

4.2. Uncertainties in SST Patterns Underpin Uncertainties in Simulations of TC Climate

Documenting the ENSO SST pattern influence on TCs using canonical CP/EP classification systems is challenging when all three last millennium simulations (MPI, CESM, LMR) yield different CP and EP SST patterns (Figure 3). We might expect that the three products would yield different storm responses (Figures 5 and 6). Over-reliance on simple binary classification systems for ENSO flavors can be problematic—especially when applied to data products beyond historical observations (e.g., Luo et al., 2022; Williams & Patricola, 2018). In LMR, for example, the SST signature for CP events appears weak in terms of temperature magnitude, but the pattern of warming is largely the same as EP events (Figures 3c and 3d). Subsequently, our analysis of TCs in LMR shows little difference in track and genesis patterns between the two types of El Niño events (Figures 5f and 6f). Previous work (Mueller et al., 2024) studying TC responses to diverse ENSO events used averaged SST patterns derived from climate model (CESM) simulations of the historical period (1980–2000) to force storm simulations (e.g., WRF). However, the CP and EP SST patterns used to force these TC simulations are not fully consistent with SST patterns from reanalysis SST patterns for ENSO events (Mueller et al., 2024). If all models simulate distinct CP and EP ENSO patterns, it may be difficult to conclusively tie these two El Niño flavors to statistically different TC outcomes.

Climate models and the data assimilation products (which rely on climate models for their spatial pattern) contain many known biases in tropical Pacific SST patterns. A known bias of data assimilation reconstructions like the LMR is a reduction in SST variance moving back in time. Proxy networks decrease back in time. As proxy information decreases, data assimilation reconstructions drift closer to the mean climate model state (Hakim et al., 2016; Tardif et al., 2019). Thus, the reduced variance in CP and EP SST patterns found in LMR may be due to proxy network biases. Additionally, many Coupled Model Intercomparison Project Phase 6 (CMIP6) climate models contain large cold tongue biases and produce artificial regularity in ENSO event frequencies (Erickson & Patricola, 2023). The month of peak ENSO response (January vs. December), the month of storm genesis, the seasonality of ENSO impacts in the Atlantic, and the underlying tropical Pacific SST pattern are all critical for North Atlantic TC teleconnections (Dong et al., 2021; Wills et al., 2022). All these features are imperfectly simulated in climate models, and thus it is difficult to disentangle the impacts of these biases on resulting synthetic TC simulations (Seager et al., 2019; Sobel et al., 2023).

Our work underscores the critical importance of refining climate model projections of future tropical Pacific SST patterns, specifically changes to El Niño SST patterns under global warming. Ultimately, it is the future tropical SST patterns that will alter TC characteristics. Many CMIP6 models project warming in the eastern tropical Pacific in the 21st century, but this robust warming pattern in climate models is not yet observed (Ceppi & Gregory, 2017; Cesana & Del Genio, 2021; Coats & Karnauskas, 2017; Fedorov et al., 2020). The correct simulation of the compounding impacts of ENSO and global warming, and of ENSO SST patterns themselves, is a necessary first step that limits our ability to study ENSO-TC connections beyond observations. Improving climate model simulations of ENSO could require incorporating smaller scale feedbacks into models including TC feedbacks on ENSO. Previous work has shown a positive feedback loop between tropical cyclones and upper ocean circulation that can help promote and maintain El Niño conditions in the tropical Pacific (Fedorov et al., 2010).

4.3. Paths to Improved Simulations of ENSO-TC Connections in a Changing Climate

Here we sort all El Niño events across four distinct data products into CP/EP-types based on indices. The use of agnostic classification methods, such as self-organizing maps (e.g., Parsons et al., 2018), could circumvent issues arising from binary classification systems and, to some extent, climate model biases. Future work could apply self-organizing maps to isolate similar SST patterns across ensembles of model simulations and observations instead of forcing each data product to conform to the EP/CP indices. Such unsupervised machine learning approaches would group physically consistent data from multiple models to reexamine the links between SST patterns and TC characteristics, perhaps avoiding some model biases.

Our study extends the statistics of ENSO and TC climate over the last millennium. An alternative approach to studying ENSO diversity in North Atlantic TCs focuses on idealized SST-forcing experiments to isolate the dynamical response to sustained SST patterns (Mueller et al., 2024; Patricola et al., 2016). Mueller et al. (2024) used a forced idealized SST pattern derived from a single climate model (CESM) to simulate ENSO impacts on TC climate. Mueller et al. (2024) found stronger TC suppression during EP years compared to CP years, suggesting that North Atlantic TCs are more effectively suppressed when tropical deep convection is located further eastward. This work matches with our past millennium results. In particular, the idealized CESM simulations produced much higher VWS (>10 m/s) during EP events than during CP, leading to greater TC suppression. In the CESM last millennium data set analyzed here, we also show higher values for VWS during EP events, but the magnitude of change is smaller (<5 m/s) (Figure 9). Unlike the idealized experiments of Mueller et al. (2024), our work cannot control for competing Atlantic climate influences on TCs. Our synthetic storm data sets respond to both ENSO teleconnections and to factors beyond ENSO, such as Atlantic SST variability (Patricola et al., 2014). Our approach, thus, makes it difficult to isolate ENSO influences on storms but does allow for exploring the wealth of TC responses that can occur during a wider variety of ENSO patterns (captured over the past millennium). The VWS response in CESM to EP events may be unique to that model, but it is possible that the mechanisms linking Atlantic VWS to ENSO are not fully resolved in current-generation climate models. If ENSO-VWS linkages are biased, improperly represented, or differ across climate models, our ability to capture TC impacts from diverse SST patterns is severely limited.

The use of idealized SST experiments is limited by the very small number of observed CP events in the satellite era (6–7), which reduces our confidence in their relevance and similarity to future warming simulations. Mueller et al. (2024) suggested a need for a suite of global model simulations to be used for statistical downscaling of storms using multiple climate models from CMIP6 (with CMIP7 forthcoming). The use of more model simulations at higher resolution has the potential to provide more meaningful connections between ENSO SST patterns and North Atlantic TC climate. We also suggest the use of a hierarchy of models used for TC downscaling based on a single climate model (to isolate the impact of WRF (Mueller et al., 2024; Patricola et al., 2016) versus statistical dynamical downscaling (Emanuel, 2006; Lee et al., 2020; Lin et al., 2023).

In summary, there remains much work to do to link observations, theory, and model simulations of ENSO-TC coupling to generate actionable projections. Our work suggests that inter-model spread in simulating ENSO-North Atlantic TC teleconnections is large. Our approach characterizes a range of different types of CP and EP events, each from a different GCM with different SST biases. Perhaps these variations provide reasonable analogs to nature; either way, we hope that this effort underscores that limitations in our simulation of realistic CP and EP El Niño patterns form a critical barrier that needs to be addressed to properly characterize future North Atlantic TC risks in a changing climate.

5. Conclusions

Constraining the relationship between ENSO and North Atlantic TCs remains an important scientific problem for improving seasonal storm predictions. The limited number of observational El Niño events and the diversity of SST patterns observed during those events make it difficult to constrain the response of North Atlantic TCs to different tropical Pacific SST patterns. Biases in earth system models, that are transferred to TC downscaling models, further compound this issue (Sobel et al., 2023). This research examines the role of ENSO diversity on Atlantic TCs over the last millennium using a set of earth system models and data assimilation reconstructions as the climate inputs. We used large sets (>100 k) of statistically-dynamically downscaled storms (Sullivan et al., 2025a; Wallace et al., 2021a, 2021b) to explore shifts in TC intensity, genesis, and track patterns. Our work shows that all last millennium climate reconstructions can produce an appropriate TC response to the canonical ENSO cycle (i.e., suppression during El Niño and enhancement during La Niña). However, SST patterns for CP and EP El Niños are expressed differently across climate models, leading to distinct ENSO-TC teleconnections.

Conflict of Interest

The authors declare no conflicts of interest relevant to this study.

Availability Statement

Synthetic storms are available at (Sullivan et al., 2025b; Wallace et al., 2021a, 2021b). All the climate data sets used in this analysis are publicly available: LMR (Parsons and Hakim, 2019), MPI (https://www.wdc-climate.de/ui/q) and CESM LME (https://www.earthsystemgrid.org).

Acknowledgments

We thank Sam Stevenson and Jiang Zhu for helpful conversations about ENSO behavior in the CESM-LME ensemble members. This work was funded by the National Science Foundation Grant P2C2-2234815 (to E. J. Wallace, G.A. Vecchi, K. A. Emanuel and S. G. Dee).

References

Ashok, K., Behera, S. K., Rao, S. A., Weng, H., & Yamagata, T. (2007). El Niño Modoki and its possible teleconnection. *Journal of Geophysical Research*, *112*(C11), 2006JC003798. https://doi.org/10.1029/2006JC003798

Bamston, A. G., Chelliah, M., & Goldenberg, S. B. (1997). Documentation of a highly ENSO-related sst region in the equatorial Pacific: Research note. *Atmosphere-Ocean*, *35*(3), 367–383. https://doi.org/10.1080/07055900.1997.9649597

Bell, G. D., & Chelliah, M. (2006). Leading tropical modes associated with interannual and multidecadal fluctuations in north Atlantic hurricane activity. *Journal of Climate*, *19*(4), 590–612. https://doi.org/10.1175/JCLI3659.1

Braconnot, P., Harrison, S. P., Kageyama, M., Bartlein, P. J., Masson-Delmotte, V., Abe-Ouchi, A., et al. (2012). Evaluation of climate models using palaeoclimatic data. *Nature Climate Change*, *2*(6), 417–424. https://doi.org/10.1038/nclimate1456

Cai, W., Wang, G., Dewitte, B., Wu, L., Santoso, A., Takahashi, K., et al. (2018). Increased variability of eastern Pacific El Niño under greenhouse warming. *Nature*, *564*(7735), 201–206. https://doi.org/10.1038/s41586-018-0776-9

Camargo, S. J., Emanuel, K., & Sobel, A. H. (2007). Use of a genesis potential index to diagnose ENSO effects on tropical cyclone genesis. *Journal of Climate*, *20*(19), 4819–4834. https://doi.org/10.1175/JCLI4282.1

Capotondi, A., Wittenberg, A., Kug, J.-S., Takahashi, K., & McPhaden, M. (2021). ENSO diversity. In *El niño southern oscillation in a changing climate* (1st ed., pp. 65–86). John Wiley and Sons, Inc.

Capotondi, A., Wittenberg, A. T., Newman, M., Di Lorenzo, E., Yu, J.-Y., Braconnot, P., et al. (2015). Understanding ENSO diversity. *Bulletin of the American Meteorological Society*, *96*(6), 921–938. https://doi.org/10.1175/BAMS-D-13-00117.1

Ceppi, P., & Gregory, J. M. (2017). Relationship of tropospheric stability to climate sensitivity and Earth's observed radiation budget. *Proceedings of the National Academy of Sciences*, *114*(50), 13126–13131. https://doi.org/10.1073/pnas.1714308114

Cesana, G. V., & Del Genio, A. D. (2021). Observational constraint on cloud feedbacks suggests moderate climate sensitivity. *Nature Climate Change*, *11*(3), 213–218. https://doi.org/10.1038/s41558-020-00970-y

Chu, P. (2004). ENSO and tropical cyclone activity. In R. J. Murnane & K. Liu (Eds.), *Hurricanes and typhoons: Past, present, and future* (pp. 297–332). Columbia University Press.

Coats, S., & Karnauskas, K. B. (2017). Are simulated and observed twentieth century tropical Pacific sea surface temperature trends significant relative to internal variability? *Geophysical Research Letters*, *44*(19), 9928–9937. https://doi.org/10.1002/2017GL074622

Dong, Y., Armour, K. C., Proistosescu, C., Andrews, T., Battisti, D. S., Forster, P. M., et al. (2021). Biased estimates of equilibrium climate sensitivity and transient climate response derived from historical CMIP6 simulations. *Geophysical Research Letters*, *48*(24), e2021GL095778. https://doi.org/10.1029/2021GL095778

Emanuel, K. (2006). Climate and tropical cyclone activity: A new model downscaling approach. *Journal of Climate*, *19*, 4797–4802. https://doi.org/10.1175/jcli3908.1

Emanuel, K., Ravela, S., Vivant, E., & Risi, C. (2006). A statistical deterministic approach to hurricane risk assessment. *Bulletin of the American Meteorological Society*, *87*(3), 299–314. https://doi.org/10.1175/BAMS-87-3-299

Emanuel, K., Sundararajan, R., & Williams, J. (2008). Hurricanes and global warming: Results from downscaling IPCC AR4 simulations. *Bulletin of the American Meteorological Society*, *89*(3), 347–367. https://doi.org/10.1175/BAMS-89-3-347

Erickson, N. E., & Patricola, C. M. (2023). Future projections of the El Niño—southern oscillation and tropical Pacific mean state in CMIP6. *Journal of Geophysical Research: Atmospheres*, *128*(21), e2022JD037563. https://doi.org/10.1029/2022JD037563

Fedorov, A. V., Brierley, C. M., & Emanuel, K. (2010). Tropical cyclones and permanent El nino in the early Pliocene Epoch. *Nature*, *463*(7284), 1066–1070. https://doi.org/10.1038/nature08831

Fedorov, A. V., Hu, S., Wittenberg, A. T., Levine, A. F. Z., & Deser, C. (2020). ENSO low-frequency modulation and mean state interactions. In M. J. McPhaden, A. Santoso, & W. Cai (Eds.), *Geophysical monograph series* (1st ed., pp. 173–198). Wiley. https://doi.org/10.1002/9781119548164.ch8

GFDL Global Atmospheric Model Development Team. (2004). The new GFDL global atmosphere and land model AM2–LM2: Evaluation with prescribed SST simulations. *Journal of Climate*, *17*(24), 4641–4673. https://doi.org/10.1175/JCLI-3223.1

Giorgetta, M. A., Jungclaus, J., Reick, C. H., Legutke, S., Bader, J., Böttinger, M., et al. (2013). Climate and carbon cycle changes from 1850 to 2100 in MPI-ESM simulations for the coupled model intercomparison project phase 5. *Journal of Advances in Modeling Earth Systems*, *5*(3), 572–597. https://doi.org/10.1002/jame.20038

Goldenberg, S. B., & Shapiro, L. J. (1996). Physical mechanisms for the association of El Niño and West African rainfall with Atlantic major hurricane activity. *Journal of Climate*, *9*(6), 1169–1187. https://doi.org/10.1175/1520-0442(1996)009<1169:PMFTAO>2.0.CO;2

Gori, A., Lin, N., Xi, D., & Emanuel, K. (2022). Tropical cyclone climatology change greatly exacerbates US extreme rainfall–surge hazard. *Nature Climate Change*, *12*(2), 171–178. https://doi.org/10.1038/s41558-021-01272-7

Gray, W. M. (1984). Atlantic seasonal hurricane frequency. Part I: El Niño and 30 mb quasi-biennial oscillation influences. *Monthly Weather Review*, *112*(9), 1649–1668. https://doi.org/10.1175/1520-0493(1984)112<1649:ashfpi>2.0.co;2

Hakim, G. J., Emile-Geay, J., Steig, E. J., Noone, D., Anderson, D. M., Tardif, R., et al. (2016). The last millennium climate reanalysis project: Framework and first results. *Journal of Geophysical Research: Atmospheres*, *121*(12), 6745–6764. https://doi.org/10.1002/2016JD024751

Hersbach, H., Bell, B., Berrisford, P., Hirahara, S., Horányi, A., Muñoz-Sabater, J., et al. (2020). The ERA5 global reanalysis. *Quarterly Journal of the Royal Meteorological Society*, *146*(730), 1999–2049. https://doi.org/10.1002/qj.3803

Kortum, G., Vecchi, G. A., Hsieh, T.-L., & Yang, W. (2024). Influence of weather and climate on multidecadal trends in Atlantic hurricane genesis and tracks. *Journal of Climate*, *37*(5), 1501–1522. https://doi.org/10.1175/JCLI-D-23-0088.1

Kossin, J. P., Camargo, S. J., & Sitkowski, M. (2010). Climate modulation of North Atlantic hurricane tracks. *Journal of Climate*, *23*(11), 3057–3076. https://doi.org/10.1175/2010JCLI3497.1

Kousky, V. E., & Higgins, R. W. (2007). An alert classification system for monitoring and assessing the ENSO cycle. *Weather and Forecasting*, *22*(2), 353–371. https://doi.org/10.1175/WAF987.1

Laloyaux, P., De Boisseson, E., Balmaseda, M., Bidlot, J., Broennimann, S., Buizza, R., et al. (2018). CERA-20C: A coupled reanalysis of the twentieth century. *Journal of Advances in Modeling Earth Systems*, *10*(5), 1172–1195. https://doi.org/10.1029/2018MS001273

Larkin, N. K., & Harrison, D. E. (2005a). Global seasonal temperature and precipitation anomalies during El Niño autumn and winter. *Geophysical Research Letters*, *32*(16), 2005GL022860. https://doi.org/10.1029/2005GL022860

Larkin, N. K., & Harrison, D. E. (2005b). On the definition of El Niño and associated seasonal average U.S. weather anomalies. *Geophysical Research Letters*, *32*(13), 2005GL022738. https://doi.org/10.1029/2005GL022738

Lee, C.-Y., Camargo, S. J., Sobel, A. H., & Tippett, M. K. (2020). Statistical–dynamical downscaling projections of tropical cyclone activity in a warming climate: Two diverging genesis scenarios. *Journal of Climate*, *33*(11), 4815–4834. https://doi.org/10.1175/JCLI-D-19-0452.1

Lee, T., & McPhaden, M. J. (2010). Increasing intensity of El Niño in the central-equatorial Pacific. *Geophysical Research Letters*, *37*(14), 2010GL044007. https://doi.org/10.1029/2010GL044007

Lin, I.-I., Camargo, S., Patricola, C., Boucharel, J., Chand, S., Klotzbach, P., et al. (2021). ENSO and tropical cyclones. In *El niño southern oscillation in a changing climate* (1st ed., pp. 377–408). John Wiley and Sons, Inc.

Lin, J., Lee, C.-Y., Camargo, S. J., Sobel, A. H., & Zhuo, J.-Y. (2025). The response of tropical cyclone hazard to natural and forced patterns of warming. *npj Climate and Atmospheric Science*, *8*(1), 109. https://doi.org/10.1038/s41612-025-00997-y

Lin, J., Rousseau-Rizzi, R., Lee, C., & Sobel, A. (2023). An open-source, physics-based, tropical cyclone downscaling model with intensity-dependent steering. *Journal of Advances in Modeling Earth Systems*, *15*(11), e2023MS003686. https://doi.org/10.1029/2023MS003686

Luo, X., Dee, S., Lavenhouse, T., Muñoz, S., & Steiger, N. (2023). Tropical Pacific and north Atlantic sea surface temperature patterns modulate Mississippi basin hydroclimate extremes over the last millennium. *Geophysical Research Letters*, *50*(2), e2022GL100715. https://doi.org/10.1029/2022GL100715

Luo, X., Dee, S., Stevenson, S., Okumura, Y., Steiger, N., & Parsons, L. (2022). Last millennium ENSO diversity and North American teleconnections: New insights from paleoclimate data assimilation. *Paleoceanography and Paleoclimatology*, *37*(3), e2021PA004283. https://doi.org/10.1029/2021PA004283

Mueller, T. J., Patricola, C. M., & Bercos-Hickey, E. (2024). The influence of ENSO diversity on future Atlantic tropical cyclone activity. *Journal of Climate*, *37*(15), 3959–3975. https://doi.org/10.1175/JCLI-D-23-0286.1

Otto-Bliesner, B. L., Brady, E. C., Fasullo, J., Jahn, A., Landrum, L., Stevenson, S., et al. (2016). Climate variability and change since 850 CE. An ensemble approach with the community Earth system model. *Bulletin of the American Meteorological Society*, *97*(5), 735–754. https://doi.org/10.1175/BAMS-D-14-00233.1

PAGES 2k-PMIP3 group. (2015). Continental-scale temperature variability in PMIP3 simulations and PAGES 2k regional temperature reconstructions over the past millennium. *Climate of the Past*, *11*(12), 1673–1699. https://doi.org/10.5194/cp-11-1673-2015

Parsons, L. A., Coats, S., & Overpeck, J. T. (2018). The continuum of drought in Southwestern North America. *Journal of Climate*, *31*(20), 8627–8643. JCLI-D-18-0010.1. https://doi.org/10.1175/JCLI-D-18-0010.1

Parsons, L. A., & Hakim, G. (2019). Data from 'local regions associated with interdecadal global temperature variability in the last millennium reanalysis and CMIP5 models [Dataset]. *Zenodo*. https://doi.org/10.5281/zenodo.5636998

Patricola, C. M., Chang, P., & Saravanan, R. (2016). Degree of simulated suppression of Atlantic tropical cyclones modulated by flavour of El Niño. *Nature Geoscience*, *9*(2), 155–160. https://doi.org/10.1038/ngeo2624

Patricola, C. M., Saravanan, R., & Chang, P. (2014). The impact of the El Niño–Southern oscillation and Atlantic meridional mode on seasonal Atlantic tropical cyclone activity. *Journal of Climate*, *27*(14), 5311–5328. https://doi.org/10.1175/JCLI-D-13-00687.1

Rasmusson, E. M., & Carpenter, T. H. (1982). Variations in tropical sea surface temperature and surface wind fields associated with the southern Oscillation/El niño. *Monthly Weather Review*, *110*(5), 354–384. https://doi.org/10.1175/1520-0493(1982)110<0354:vitsst>2.0.co;2

Sabin, T. P., Babu, C. A., & Joseph, P. V. (2013). SST–Convection relation over tropical oceans. *International Journal of Climatology*, *33*(6), 1424–1435. https://doi.org/10.1002/joc.3522

Seager, R., Cane, M., Henderson, N., Lee, D.-E., Abernathey, R., & Zhang, H. (2019). Strengthening tropical Pacific zonal sea surface temperature gradient consistent with rising greenhouse gases. *Nature Climate Change*, *9*(7), 517–522. https://doi.org/10.1038/s41558-019-0505-x

Shin, N.-Y., Kug, J.-S., Stuecker, M. F., Jin, F.-F., Timmermann, A., & Kim, G.-I. (2022). More frequent central Pacific El niño and stronger eastern Pacific El Niño in a warmer climate. *npj Climate and Atmospheric Science*, *5*(1), 101. https://doi.org/10.1038/s41612-022-00324-9

Sobel, A. H., Lee, C.-Y., Bowen, S. G., Camargo, S. J., Cane, M. A., Clement, A., et al. (2023). Near-term tropical cyclone risk and coupled Earth system model biases. *Proceedings of the National Academy of Sciences*, *120*(33), e2209631120. https://doi.org/10.1073/pnas.2209631120

Stevenson, S., Capotondi, A., Fasullo, J., & Otto-Bliesner, B. (2019). Forced changes to twentieth century ENSO diversity in a last millennium context. *Climate Dynamics*, *52*(12), 7359–7374. https://doi.org/10.1007/s00382-017-3573-5

Sullivan, R., Wallace, E., Dee, S., Vecchi, G., Yang, W., & Kerry, E. (2025b). Multi-centennial spatial coherency among Atlantic tropical cyclones from simulated and reconstructed storm records—Storm dataset and code [Dataset]. *Zenodo*. https://doi.org/10.5281/zenodo.15262056

Sullivan, R. M., Wallace, E., Dee, S., Vecchi, G. A., Yang, W., & Emanuel, K. (2025a). Multi-centennial spatial coherency among Atlantic tropical cyclones from simulated and reconstructed storm records. *Geophysical Research Letters*, *52*(18), e2025GL116642. https://doi.org/10.1029/2025GL116642

Takahashi, K., Montecinos, A., Goubanova, K., & Dewitte, B. (2011). ENSO regimes: Reinterpreting the canonical and modoki El Niño: Reinterpreting enso modes. *Geophysical Research Letters*, *38*(10). https://doi.org/10.1029/2011GL047364

Tang, B. H., & Neelin, J. D. (2004). ENSO influence on Atlantic hurricanes via tropospheric warming. *Geophysical Research Letters*, *31*(24), 2004GL021072. https://doi.org/10.1029/2004GL021072

Tardif, R., Hakim, G. J., Perkins, W. A., Horlick, K. A., Erb, M. P., Emile-Geay, J., et al. (2019). Last millennium reanalysis with an expanded proxy database and seasonal proxy modeling. *Climate of the Past*, *15*(4), 1251–1273. https://doi.org/10.5194/cp-15-1251-2019

Ting, M., Kossin, J. P., Camargo, S. J., & Li, C. (2019). Past and future hurricane intensity change along the U. S. east Coast. *Scientific Reports*, *9*(7795), 1–8. https://doi.org/10.1038/s41598-019-44252-w

Vecchi, G. A., Delworth, T. L., Gudgel, R., Kapnick, S., Rosati, A., Wittenberg, A. T., et al. (2014). On the seasonal forecasting of regional tropical cyclone activity. *Journal of Climate*, *27*(21), 7994–8016. https://doi.org/10.1175/JCLI-D-14-00158.1

Villarini, G., Vecchi, G. A., & Smith, J. A. (2010). Modeling the dependence of tropical storm counts in the north Atlantic basin on climate indices. *Monthly Weather Review*, *138*(7), 2681–2705. https://doi.org/10.1175/2010MWR3315.1

Waliser, D. E., Graham, N. E., & Gautier, C. (1993). Comparison of the highly reflective cloud and outgoing longwave radiation datasets for use in estimating tropical deep convection. *Journal of Climate*, *6*(2), 331–353. https://doi.org/10.1175/1520-0442(1993)006<0331:cothrc>2.0.co;2

Wallace, E. J., Dee, S. G., & Emanuel, K. A. (2021a). Building pseudo proxy paleotempestology networks using synthetic north Atlantic tropical cyclones [Dataset]. *Zenodo*. https://doi.org/10.5281/zenodo.4959615

Wallace, E. J., Dee, S. G., & Emanuel, K. A. (2021b). Resolving long-term variations in North Atlantic tropical cyclone activity using a pseudo proxy paleotempestology network approach. *Geophysical Research Letters*, *48*(18), 1–13. https://doi.org/10.1029/2021gl094891

Williams, I. N., & Patricola, C. M. (2018). Diversity of ENSO events unified by convective threshold sea surface temperature: A nonlinear ENSO index. *Geophysical Research Letters*, *45*(17), 9236–9244. https://doi.org/10.1029/2018GL079203

Wills, R. C. J., Dong, Y., Proistosecu, C., Armour, K. C., & Battisti, D. S. (2022). Systematic climate model biases in the large-scale patterns of recent sea-surface temperature and sea-level pressure change. *Geophysical Research Letters*, *49*(17), e2022GL100011. https://doi.org/10.1029/2022GL100011

Wyrtki, K. (1975). El niño—the dynamic response of the equatorial Pacific Ocean to atmospheric forcing. *Journal of Physical Oceanography*, *5*(4), 572–584. https://doi.org/10.1175/1520-0485(1975)005<0572:entdro>2.0.co;2

Yang, W., Wallace, E., Vecchi, G. A., Donnelly, J. P., Emile-Geay, J., Hakim, G. J., et al. (2024). Last millennium hurricane activity linked to endogenous climate variability. *Nature Communications*, *15*(1), 816. https://doi.org/10.1038/s41467-024-45112-6

Yeh, S.-W., Kug, J.-S., Dewitte, B., Kwon, M.-H., Kirtman, B. P., & Jin, F.-F. (2009). El niño in a changing climate. *Nature*, *461*(7263), 511–514. https://doi.org/10.1038/nature08316

Yu, J.-Y., & Zou, Y. (2013). The enhanced drying effect of central-pacific El Niño on US winter. *Environmental Research Letters*, *8*(1), 014019. https://doi.org/10.1088/1748-9326/8/1/014019

References From the Supporting Information

Anderson, D. M., Tardif, R., Horlick, K., Erb, M. P., Hakim, G. J., Noone, D., et al. (2019). Additions to the last millennium reanalysis multi-proxy database. *Data Science Journal*, *18*(1), 2. https://doi.org/10.5334/dsj-2019-002

Balsamo, G., Beljaars, A., Scipal, K., Viterbo, P., Van Den Hurk, B., Hirschi, M., & Betts, A. K. (2009). A revised hydrology for the ECMWF model: Verification from field site to terrestrial water storage and impact in the integrated forecast system. *Journal of Hydrometeorology*, *10*(3), 623–643. https://doi.org/10.1175/2008JHM1068.1

Bonavita, M., Hólm, E., Isaksen, L., & Fisher, M. (2016). The evolution of the ECMWF hybrid data assimilation system. *Quarterly Journal of the Royal Meteorological Society*, *142*(694), 287–303. https://doi.org/10.1002/qj.2652

Bouillon, S., Morales Maqueda, M. Á., Legat, V., & Fichefet, T. (2009). An elastic–viscous–plastic sea ice model formulated on arakawa B and C grids. *Ocean Modelling*, *27*(3–4), 174–184. https://doi.org/10.1016/j.ocemod.2009.01.004

Cram, T. A., Compo, G. P., Yin, X., Allan, R. J., McColl, C., Vose, R. S., et al. (2015). The international surface pressure databank version 2. *Geoscience Data Journal*, *2*(1), 31–46. https://doi.org/10.1002/gdj3.25

Deser, C., Phillips, A. S., Tomas, R. A., Okumura, Y. M., Alexander, M. A., Capotondi, A., et al. (2012). ENSO and Pacific decadal variability in the community climate system model version 4. *Journal of Climate*, *25*(8), 2622–2651. https://doi.org/10.1175/JCLI-D-11-00301.1

Emanuel, K., DesAutels, C., Holloway, C., & Korty, R. (2004). Environmental control of tropical cyclone intensity. *Journal of the Atmospheric Sciences*, *61*(7), 843–858. https://doi.org/10.1175/1520-0469(2004)061<0843:ECOTCI>2.0.CO;2

Hou, M., & Tang, Y. (2022). Recent progress in simulating two types of ENSO – From CMIP5 to CMIP6. *Frontiers in Marine Science*, *9*, 986780. https://doi.org/10.3389/fmars.2022.986780

Hurrell, J. W., Holland, M. M., Gent, P. R., Ghan, S., Kay, J. E., Kushner, P. J., et al. (2013). The community Earth system model: A framework for collaborative research. *Bulletin of the American Meteorological Society*, *94*(9), 1339–1360.

Jungclaus, J. H., Fischer, N., Haak, H., Lohmann, K., Marotzke, J., Matei, D., et al. (2013). Characteristics of the ocean simulations in the max planck institute ocean model (MPIOM) the ocean component of the MPI-earth system model. *Journal of Advances in Modeling Earth Systems*, *5*(2), 422–446. https://doi.org/10.1002/jame.20023

Komen, G. J. & Hasselmann, K. (Eds.) (1996)., *Dynamics and modelling of ocean waves* (1. paperback ed. (with corrections))). Cambridge Univ. Press.

Landrum, L., Otto-Bliesner, B. L., Wahl, E. R., Conley, A., Lawrence, P. J., Rosenbloom, N., & Teng, H. (2013). Last millennium climate and its variability in CCSM4. *Journal of Climate*, *26*(4), 1085–1111. https://doi.org/10.1175/JCLI-D-11-00326.1

Madec, G. (2008). *NEMO ocean engine (27 ISSN No 1288–1619; Note Du Pole de Modélisation)*. Institut Pierre-Simon Laplace.

Reick, C. H., Raddatz, T., Brovkin, V., & Gayler, V. (2013). Representation of natural and anthropogenic land cover change in MPI-ESM. *Journal of Advances in Modeling Earth Systems*, *5*(3), 459–482. https://doi.org/10.1002/jame.20022

Stevenson, S., Otto-Bliesner, B., Fasullo, J., & Brady, E. (2016). "El Niño Like" hydroclimate responses to last millennium volcanic eruptions. *Journal of Climate*, *29*(8), 2907–2921. https://doi.org/10.1175/JCLI-D-15-0239.1

Schmidt, G. A., Jungclaus, J. H., Ammann, C. M., Bard, E., Braconnot, P., Crowley, T. J., et al. (2012). Climate forcing reconstructions for use in PMIP simulations of the last millennium (V1.1). *Geoscientific Model Development*, *5*(1), 185–191. https://doi.org/10.5194/gmd-5-185-2012

Schneck, R., Reick, C. H., & Raddatz, T. (2013). Land contribution to natural CO_2 variability on time scales of centuries. *Journal of Advances in Modeling Earth Systems*, *5*(2), 354–365. https://doi.org/10.1002/jame.20029

Steiger, N. J., Hakim, G. J., Steig, E. J., Battisti, D. S., & Roe, G. H. (2014). Assimilation of time-averaged pseudoproxies for climate reconstruction. *Journal of Climate*, *27*(1), 426–441. https://doi.org/10.1175/JCLI-D-12-00693.1

Stevens, B., Giorgetta, M., Esch, M., Mauritsen, T., Crueger, T., Rast, S., et al. (2013). Atmospheric component of the MPI-M Earth system model: ECHAM6. *Journal of Advances in Modeling Earth Systems*, *5*(2), 146–172. https://doi.org/10.1002/jame.20015

Woodruff, S. D., Worley, S. J., Lubker, S. J., Ji, Z., Eric Freeman, J., Berry, D. I., et al. (2011). ICOADS release 2.5: Extensions and enhancements to the surface marine meteorological archive. *International Journal of Climatology*, *31*(7), 951–967. https://doi.org/10.1002/joc.2103